Photon Anti-Bunching Properties of the Anti-Jaynes-Cummings Model

By

Patrick Muga Owiny

A thesis submitted in partial fulfillment of the requirements for the degree of master of science in theoretical physics

School of Physical & Biological Sciences

MASENO UNIVERSITY

Declaration

I, Patrick Muga Owiny, declare that this thesis titled, "*Photon Anti-Bunching Properties of the Anti-Jaynes-Cummings model*" and the work presented in it are my own. I confirm that it has not been presented for degree award in any university whatsoever.

Patrick Muga Owiny,
MSC/SC/00015/2017

Signed: ________________________

Date: ________________________

Approved By Supervisors:

1. Prof. Joseph Akeyo Omolo,
   Department of Physics & Materials Science,
   Maseno University.
   Signed: ________________________

   Date: ________________________

2. Dr. Onyango Stephen Okeyo,
   Department of Physics & Materials Science,
   Maseno University.
   Signed: ________________________

   Date: ________________________

Acknowledgment

I would like to thank the almighty God for his Grace and Blessings which has led to the completion of this research. It has been a long journey since I embarked on it and there were days when I struggled for motivation.

I extend my gratitude to my loving mother and best friend, Seline Owiny who has tirelessly made efforts to see to it that I succeed in all my endeavors and has been there for me always ever since I started my research till the end. Our mother is the beacon of the family, she is always there for us, for me. I can always lean on her shoulder and cry. Many times during the research I did.

I acknowledge the priceless coaching and guidance by my supervisors Prof. Joseph Akeyo Omolo and Dr. Onyango Stephen Okeyo under whose supervision this work was prepared. Allow me also extend my appreciation to Mr. Ongwen Nicholas and Mr. Christopher Mayero, dearest brother James Owiny and his dearest wife Debra Owiny, dearest sister Suzzy Owiny for their ceaseless moral and financial support and finally to my beloved brothers and sisters Godfrey,George,Julius,Carolyne and Willis, in-laws, nephews and niece for their ceaseless encouragement and support. Any shortcoming in this work can only be my own personal failing.

Dedication

I dedicate this work to my late dad Sir. Edward Francis Owiny Olenyo, what a untimely departure dad. Finally to the love of my life Carol Mambia Luo Otieno.

Abstract

This thesis present anti-Jaynes interaction, an interaction where anti-rotating light mode couples to a two-level atom. The anti-bunching properties of the anti-Jaynes-Cummings model was explicitly demonstrated, a model which researchers have always shied away from studying due to the notion that it was non-energy conserving. The energy conservation property was recently addressed hence creating a wider gap which need to be addressed. The anti-Jaynes-Cummings interaction was redefined as a generator of the anti-polariton qubit. Anti-polariton qubit is a two-state quantized particle specified by state vectors, Hamiltonian, conserved excitation number, identity, state transition, U(1) symmetry operators. Formation of anti-polariton qubit involves absorption or emission of negative energy photon by field mode triggered by initial emission or absorption of negative energy photon by the atom. Superposition of qubit state vectors provides the eigenvectors and eigenvalues of the anti JC Hamiltonian. The mean photon number, photon number fluctuation, density operator and atomic inversion are easily evaluated. The result of the mean and its fluctuation were used in the Mandel operator to explicitly demonstrate the anti-bunching properties of the anti-JC interaction. Exact solution of the long standing problem is of importance in understanding the statistical properties and physical properties of the interacting two level atom system which shall be of great importance in the optimization of the technological application, especially in the emerging areas of quantum teleportation and quantum computing. Attention can now be refocused in studying the practical application of the anti JC model such as quantum computing.

Contents

List of Abbreviations

JC	Jaynes-Cummings
JCM	Jaynes-Cummings model
RWA	Rotating wave approximation

List of Figures

Chapter 1

Background Information

1.1 Introduction

A simple system which has two energy levels is called a two-level atom (also known as a two-state system). The two states are described by two eigen-states $|a\rangle$ and $|b\rangle$ [1–7]. In the following sections, the various models that describe the interaction between the two-level atom and the optical fields are discussed.

1.2 The Rabi Model

The Rabi model [8] describes an atom that interacts with harmonic electric field. It is realized by injecting an atom into an electromagnetic cavity [9]. The Rabi model is associated by the Hamiltonian

$$H_R = \hbar\,\omega \left(\hat{c}^\dagger \,\hat{c} + \frac{1}{2} \right) + \hbar\,\omega_o\,\Omega_z + \hbar\,g\,(\,\hat{c}^\dagger + \hat{c}\,)\,(\,\Omega_- + \Omega_+\,)\,. \tag{1.2.1}$$

where ω , ω_o are the respective field mode and atomic spin state angular frequencies while g is the atom-field coupling constant. The coupling constant represents the strength of the atom-field coupling.

For field mode in standard number (fork) state $|n\rangle$, $\hat{c}$, $\hat{c}^\dagger$ are the respective creation and annihilation operators, lowering or raising the number state according to:

$$\hat{c}|n\rangle] = \sqrt{n}|n-1\rangle \quad ; \quad \hat{c}^+|n\rangle] = \sqrt{n+1}|n+1\rangle \tag{1.2.2}$$

while for the atom in the excited spin state $|u\rangle$ or ground state $|d\rangle$. Ω_-, Ω_+, Ω_z are the spin state lowering ,raising and population inversion operators respectively acting on the spin state according to:

$$|d\rangle = \begin{pmatrix} 0 \\ 1 \end{pmatrix} \ ; \ |u\rangle = \begin{pmatrix} 1 \\ 0 \end{pmatrix} \tag{1.2.3}$$

$$\Omega_z = \frac{1}{2}\hbar|u\rangle\langle u| - |d\rangle\langle d| \quad ; \quad \Omega_+ = \hbar|u\rangle\langle d| \quad ; \quad \Omega_- = \hbar|d\rangle\langle u|$$

$$\Omega_-|d\rangle = 0 \ ; \ \Omega_+|u\rangle = 0 \ ; \ \Omega_+|d\rangle = |u\rangle \ ; \ \Omega_-|u\rangle = |d\rangle$$

$$\Omega_z|u\rangle = \frac{1}{2}|u\rangle \ ; \ \Omega_z|d\rangle = -\frac{1}{2}|d\rangle \tag{1.2.4}$$

The Rabi model accurately describes the dynamical properties of a wide variety of systems in quantum optics and solid state models. Moreover a variety of protocols in modern information theory [10] employ the quantum Rabi model as a fundamental building block with plausible technologies [11–17].

The time-dependent Schrödinger equation governing the time evolving dynamics of the Rabi interaction would be solved directly through simple integration with respect to time, but the resulting time evolution operator is not exactly evaluated in explicit form therefore, only approximate solutions of the time-dependent Schrödinger equation for the dynamics generated by the Rabi Hamiltonian have so far been obtained explicitly. However, exact analytical solution have been obtained explicitly in the rotating wave approximation(RWA), which assumes that the interaction is very weak so that the constant g is very small in comparison to the field mode and atomic angular frequency ω and ω_o. In RWA, the Rabi Hamiltonian is reduced to only one component in which the interaction conserves energy called Jaynes-Cummings model(JCM) discussed in the next section.

1.3 Jaynes-Cummings Model

A simple but exactly solvable model called the Jaynes-Cummings model was introduced by Jaynes and Cummings [18] to consider a single two-level atom interacting with a single-mode field. Through the RWA, the $2H_R$ reduces to the JC Hamiltonian. Since the ground state energy does not generate any dynamical evolution we drop it. The field mode Hamiltonian from Eq. (1.2.1) is expressed in the form

$$\hbar\omega\left(\hat{c}^{\dagger}\hat{c}+\frac{1}{2}\right)=\frac{1}{2}\hbar\omega\left(\hat{c}^{\dagger}\hat{c}+\hat{c}\hat{c}^{\dagger}\right) \tag{1.3.1}$$

which gives

$$\hbar\omega\left(\hat{c}^{\dagger}\hat{c}+\frac{1}{2}\right)=\frac{1}{2}\hbar\omega\hat{c}^{\dagger}\hat{c}+\frac{1}{2}\hbar\omega\hat{c}\hat{c}^{\dagger} \tag{1.3.2}$$

while the free atomic spin is symmetrized to take the form

$$\hbar\omega_0\Omega_z=\frac{1}{2}\hbar\omega\Omega_z+\frac{1}{2}\hbar\omega\Omega_z \tag{1.3.3}$$

Substituting Eq. (1.3.2) and Eq. (1.3.3) into Eq. (1.2.1) and collecting the normal order terms gives the JC Hamiltonian in the form

$$H_{JC}=\hbar\,\omega\,\hat{c}^{\dagger}\,\hat{c}+\hbar\,\omega_o\,\Omega_z+2\,\hbar\,g\,(\hat{c}\,\Omega_+\;+\;\hat{c}^{\dagger}\Omega_-)\,. \tag{1.3.4}$$

The JCM has over the years attracted a lot of interest because of its energy conserving nature. In the JCM, the quantized field mode is represented by the positive frequency component in which the wave propagation is identified with the rotation in the clockwise sense and both the atom and field conserves the total excitation number [19]. The normally ordered excitation number operator is identified as

$$\hat{N}=\hat{c}^{\dagger}\,\hat{c}+\Omega_+\Omega_- -\frac{1}{2}. \tag{1.3.5}$$

The JCM is exactly solvable because of the presence of the conserved excitation number operator $\hat{N}$. Because of its conserved nature, the dynamics generated by the JC Hamiltonian is exactly solvable since it is possible to apply the conservation principle to reorganize the JC Hamiltonian in a diagonal form, in which the resulting time-dependent Schrödinger equation is exactly solvable through simple integration. Other alternative solutions [20] are also possible still based on the conservation principle. We observe that the component of the Rabi Hamiltonian Eq. (1.2.1) which is ignored in the RWA is identified with rotation in the anticlockwise sense is discussed in the next section.

1.4 Anti Jaynes-Cummings model

The property that the counter rotating component of the Rabi Hamiltonian operate in a sense which is reverse relative to the JC Hamiltonian leads to the reference anti JCM.

Substituting Eq. (1.3.2) and Eq. (1.3.3) into Eq. (1.2.1) and collecting the anti-normal order terms gives the anti JC Hamiltonian in the form

$$H_{aJC} = \hbar\omega\hat{c}\hat{c}^{+} + \hbar\omega_o\Omega_z + 2\hbar g(\hat{c}\Omega_- + \hat{c}^{+}\Omega_+). \tag{1.4.1}$$

After explicit symmetrization of the Rabi Hamiltonian in terms of the normal and anti-normal form in Eq. (1.3.4) and Eq. (1.4.1). The Rabi Hamiltonian in Eq. (1.2.1) take the form

$$H_R = \frac{1}{2}\left(H_{JC} \, + \, H_{aJC} \right). \tag{1.4.2}$$

As we have observed above, the common experience in quantum optics over the years has been that only the Jaynes-Cummings model represented by the JC Hamiltonian Eq. (1.3.4) is exactly solvable while the dynamics generated by the anti JCM is not exactly solvable always believing that it generates non-energy conserving dynamics. However, the energy conservation property of the anti JC Hamiltonian was established in the recent work in [21], where the existence of energy conservation property was explicitly demonstrated. It is this specific proof of energy conservation that has stirred the interest in the anti Jaynes-Cummings interaction [22].

Recent development on the Rabi model was the introduction of the polariton and anti-polariton terms where polariton involves emission of positive energy photon by the field mode and anti-polariton involves absorption or emission of negative energy photon by the field mode. Polariton or anti-polariton is defined as a two-state quantized particle specified by two state vectors, Hamiltonian, conserved excitation number, state transition operator, U(1) symmetry operator, SU(2) or U(1) symmetry operator and SU(1,1) symmetry operator.

Polariton and anti-polariton are obtained through appropriate re-definitions of the JC and anti JC Hamiltonian respectively [23]. The polariton qubit Hamiltonian takes the form

$$H = \hbar\omega\hat{A}^2 + \hbar g\hat{A} - \frac{\hbar}{4}\omega\alpha^2 - \frac{1}{2}\hbar\omega \;\; ; \;\; \hat{A} = \alpha\Omega_z + \hat{c}\Omega_+ + \hat{c}^{+}\Omega_- \; ; \; \alpha = \frac{\delta}{g} \; ; \; \delta = \omega_o + \omega \tag{1.4.3}$$

while the anti-polariton qubit Hamiltonian is expressed as

$$\bar{H} = \hbar\omega\hat{\bar{A}}^2 + \hbar g\hat{\bar{A}} - \frac{\hbar}{4}\omega\overline{\alpha}^2 - \frac{1}{2}\hbar\omega \;\; ; \;\; \hat{\bar{A}} = \overline{\alpha}\Omega_z + \hat{c}\Omega_- + \hat{c}^{+}\Omega_+ \; ; \; \overline{\alpha} = \frac{\overline{\delta}}{g} \; ; \; \delta = \omega_o - \omega \tag{1.4.4}$$

where $\hat{A}$ is the polariton qubit state transition operator and $\hat{\bar{A}}$ is the anti-polariton qubit state transition operator. With this transition operator one can easily determine the JC qubit state vectors as well as the anti JC qubit state vectors leading to a simple determination of eigen state vectors through superposition of the qubit state vectors and also determining the eigenvalue equation. The anti JC Hamiltonian is reorganized in the form

$$\bar{H} = \hbar\omega(n + \frac{1}{2})\hat{\bar{I}} + \hbar\bar{R}_{n+1}\hat{\bar{\varepsilon}}. \quad ; \quad \bar{R}_{n+1}(t) = \sqrt{\delta^2 + 16g^2(n+1)} \tag{1.4.5}$$

In this thesis, we study the statistical properties of a two-level atom interacting with a single quantized field mode in the anti JC model.

1.5 Statement of the problem

The anti-bunching properties of the anti JC model has never been studied due to its non-energy conservation property. The energy conservation property of the anti JC Hamiltonian was only established recently[23], conservation of the excitation number operator means that it is energy conserving and it should be specified by eigenvectors and eigenvalues just like it has been done for the Jaynes-Cummings interaction. The proof of energy conservation made it clear that the model is solvable, the anti JC has stirred interests in the recent past. We study the photon anti-bunching properties of the anti JC model. Where photon anti-bunching by definition is the process through which photons are produced one by one.

1.6 Objectives of the study

The general objective of this study is to describe the anti-bunching property of a two-level atom interacting with a quantized electromagnetic field mode (anti Jaynes-Cummings model) without using the rotating wave approximation. The specific objectives are to determine the:

1. Mean photon number and fluctuations.
2. Atomic spin population inversion in the state $|\Psi(t)\rangle$.
3. Fluctuation in the atomic inversion.
4. Density operator and purity of state.

1.7 Significance of the study

An exact solution of the long outstanding problem provided clearer understanding of the statistical properties and physical features of the anti JC model. Results obtained will be of much importance in optimizing technological applications of the model especially in the emerging areas of quantum computation and quantum teleportation.

Chapter 2

Literature Review

A lot of work [22, 24–26] has been done towards understanding the internal dynamics and physical properties of a two-level atom interacting with a single mode of quantized electromagnetic field, formulated as a quantum Rabi model with Hamiltonian H_R in Eq. (1.2.1).

An exact analytical solution of the time-dependent Schrödinger equation describing the time evolving states of the Rabi model has never been determined and has over the years remained a major challenge. This long standing problem may be attributed to the approximate nature of the Rabi model, which is based on the electric dipole approximation or to the non-commutative algebraic properties of the model Hamiltonian H_R.

The difficulty to obtain an exact analytical solution describing the dynamical evolution of the Rabi model led to a reformulation of the Rabi Hamiltonian in exactly solvable approximate form [18]. The remainder of the chapter is organized as follows. The Rabi model is discussed in section 2.1, followed by the review of the Jaynes-Cummings model (JCM) in section 2.2 and anti JCM in section 2.3.

2.1 The Rabi Model

The Rabi model constitutes probably the simplest physical system beyond the harmonic oscillator. Its applications range from quantum optics [20, 27–30], magnetic resonance [31–34] to molecular physics [35]. The model has also gained a prominent role in novel fields of research such as cavity quantum electrodynamics [36, 37].

Several attempts have been made towards solving the Rabi model. One of the approaches is described in [38] where the energy spectrum of the Rabi Hamiltonian is obtained using Bargmann-space formalism [24] where the field annihilation and creation operators are converted into C-number variables. The exact spectrum of the Rabi Hamiltonian for arbitrary coupling strength and detuning are then analytically determined. The work in Ref. [38] also demonstrated the criteria for integrability of quantum systems containing discrete degrees of freedom. To this end, the phenomenological level-labeling criterion of quantum integrability proposed in [38] satisfies the quantum Rabi model and the approach yields the energy eigenspectrum of the Rabi model. Despite the success of the method in [38], the results obtained for eigenvalues and eigenstates spectrum are complicated making it difficult to use them to obtain the general time evolution of the Rabi model.

Specification of the full spectrum of the classical Rabi system has also been done after the work of [39], where the Bargmann-Fock Hilbert space $\mathfrak{R}$ was applied. This is a space of entire functions of one complex variable with a scalar product. In the approach, the Rabi model turns out to be a quasi-exactly solvable model. The concept of quasi-exact solvability applies to a quantum system for which only part of the eigen spectrum can be derived algebraically [40, 41]. For the quantum Rabi model, this is exceptional part of the eigen spectrum made up of the isolated exact Judd points, which can be derived algebraically, among a number of different approaches.

Eq. (1.2.1) posses a serious obstruction to its analytical solutions because of the apparent lack of second conserved quantity [18] besides the energy conservation which has led to widespread opinion that it is not integrable. To remedy this difficulty, Jaynes and Cummings proposed the rotating wave approximation (RWA) [18]. This approximation assumes that the interaction is very weak and the coupling constant g is very small in comparison to the field mode and atomic spin angular frequencies ω and ω_o. In the rotating wave approximation, the Rabi model is reduced to a solvable JCM, discussed in the following section.

2.2 The Jaynes-Cummings Model

The Jaynes-Cummings model [18] was introduced to describe the interaction between a two-level atom and quantized electromagnetic field. The JCM is obtained from the Rabi model by the RWA which is justified for small detuning. The JCM has been useful in describing various physical phenomenon such as collapse-revivals [25, 42], Rabi oscillations [43] and atom-field entanglement [16, 22, 44]. Within the RWA, the JCM has been studied in two different pictures, the Schrödinger picture [20] and the Heisenberg picture [45]. In the Schrödinger dimension, the exact solution of the JCM can be obtained [20] and the Rabi oscillation predicted with the solution proof of the population inversion. Since the JCM proved to be solvable, this was a clear indication that the JCM has algebraic expression for probability amplitudes [20]. In the Heisenberg picture [45], it was shown that the model permits simple expressions for the solutions of the Heisenberg equations [46].

The JCM has also been used to get the density operator [47]. Density operator is then used to get the Bloch vector which is useful in describing the state of an atom. For a pure atom state, the Bloch vector has a unit length and hence move on a sphere of unit length while mixed state has a shorter vector.

Photon number state of the JCM has also been investigated in [48] and the result is a direct proof that during the JC interaction, there is periodic exchange of energy between the field and the atom and that the oscillation of the field energy is given by the mean photon number.

The statistical properties of the JCM has been investigated using the Mandel-Q operator [49], which measures how the field differs from the classical field [48]. The Mandel-Q operator explains the boundary process such that when $Q > 0$, then the photon is interpreted to be bunched but when $Q < 0$, the photon is anti-bunched hence sub-Poissonian statistics, which is purely quantum in nature [49].

The expectation values of the quadrature operators of the JCM has been studied where it was noted that when the variance is less than $\frac{1}{4}$ then the field is squeezed [50].

However, experimental observations have revealed that some effects such as atom-cavity entanglement [44] are not accounted for in the RWA [51]. This limitation led to the study of Rabi model in improved RWA [52]. In the improved RWA, the dynamics of the Rabi model is studied numerically by subjecting it to a dissipative effect acting only on both the atom and the cavity mode. It came out that the anti-rotating term of the Rabi model induces photon creation of the vacuum which is interpreted using quantum trajectory approach and macroscopic ad hoc model of dephasing based on stochastic oscillations of the atomic transition frequency. It was evident that the photon creation through atomic decoherence [48, 53] is suppressed in the presence of damping mechanism and estimated the magnitude of this phenomenon using current experimental values of parameters, noting that the phenomenon might become relevant in future experiments.

The JCM has also been explicitly studied by subjecting it to a strong coupling regime [26, 54], i. e., a regime where the RWA does not apply. Under this regime, the RWA breaks down and Rabi model becomes analytically unsolvable.

In strong coupling regime [26], the photon number wave packets propagate coherently along two independent chains, where they generates counter-propagating photon number wave-packets in both directions. The results are full collapse and partial revivals where probability is not restored. The collapses and revivals have interesting consequences in phase space which is analyzed using Wigner function [55] and phase space trajectories [24].

The counter-rotating terms have also been shown to have profound effect on the long time behavior of the system since by including them in the semi-classical equations lead to chaotic behavior [56]. The solution of the JCM with the counter rotating terms have been presented under weak coupling regimes and a small dependence of the atomic inversion arising from interference.

It was later considered that the anti JCM may be responsible for such experimental effects leading to the interpretation that those effects are associated with anti JC components which are dropped in the approximation. The anti JCM is discussed in the next section.

2.3 The anti Jaynes-Cummings Model

The long outstanding problem of conserved excitation number operator of the anti JC model was explicitly addressed in Ref. [21] using operator ordering a fundamental algebraic property to determine the conserved nature of the excitation number operator and U(1) symmetry operator for the rotating and anti-rotating of the Rabi model.

The determination of $\hat{\bar{N}} = \hat{c}\hat{c}^{+} + \Omega_{-}\Omega_{+}$ using the principle of operator ordering was enough proof that the anti JCM is solvable. In the work described in Ref. [21], the anti JC Hamiltonian is reorganized in the form

$$\bar{H} = \hbar\omega(\hat{c}\hat{c}^{+} + \Omega_{-}\Omega_{+}) + 2\hbar g(\bar{\alpha}\Omega_{z} + \hat{c}\Omega_{-} + \hat{c}^{+}\Omega_{+}) - \frac{1}{2}\hbar\omega; \quad \bar{\alpha} = \frac{\omega_{o} - \omega}{2g} \tag{2.3.1}$$

where the symbols have their usual meaning. It was explicitly shown in [21] that the Rabi Hamiltonian is composed of two algebraically complete JC and anti JC components each specified by its characteristic excitation number, state transition, u(1)-symmetry and red and blue side-band eigenvalue spectrum.

The realization that the excitation number operator of the anti JC model is conserved has sparked interest in the study of the anti JC model [22]. Even though it was a great achievement, the dynamical properties of the JC model was never investigated hence leaving a wider gap which needs to be bridged. The precise algebraic and physical framework for studying the dynamics and practical applications of polariton and anti-polariton qubits[23], interpreted as a two-state quantized particles formed through the coupling of an atomic spin to a rotating positive frequency or anti-rotating negative frequency component of the quantized electric field was developed [23]. The quantum Rabi optical lattice was taken as a geometrical framework for studying the dynamics and physical properties of systems of interacting polariton and anti-polariton qubits.

The conserved nature of the anti JC Hamiltonian was again proved by introducing a state transition operator given by

$$\hat{\bar{A}} = \bar{\alpha}\Omega_{z} + \hat{c}\Omega_{-} + \hat{c}^{\dagger}\Omega_{+} \tag{2.3.2}$$

which gave the reformulated anti-Jaynes-Cummings Hamiltonian

$$\bar{H} = \hbar\omega\hat{\bar{N}} + 2g\hat{\bar{A}} - \frac{1}{2}\hbar\omega. \tag{2.3.3}$$

The only studies which so far has been done on the anti JCM are the proof of the conserved nature of the excitation number operator [21], obtaining its eigenvectors and eigenvalues [23] and the Rabi oscillations, entanglement and teleportation of the anti JCM [22] are the only studies which have so far been done explicitly on the model. But the specific studies of the statistical properties like determination of the time development of the photon number and obtaining the density matrix have not been studied.

Chapter 3

Research Methodology

We started by noting that within Schrödinger picture the state vectors evolve in time but the operators are constant with time while in the Heisenberg picture the states are constant while operators evolve in time whereas within the interaction picture both state and operators evolve in time. Our method involves the analysis of the anti JC Hamiltonian. We use direct integration method within the Schrödinger picture since the anti JC Hamiltonian is time independent. Since the Rabi Hamiltonian has been expressed in terms of the JC and anti JC Hamiltonian in Eq. (1.3.4) and Eq. (1.4.1) [23], by introducing normal and anti-normal operator ordering respectively, we consider the lower Rabi subspace, subspace where the interaction begins with the atom in an initial spin-down state $|d\rangle$ and the field mode in an initial number state $|n\rangle$ such that the polariton and anti-polariton qubit [21] is formed in an initial n-photon spin-down state $|\Psi_{nd}\rangle$ defined by

$$|\Psi_{nd}\rangle = |nd\rangle$$

We redefine anti JC Hamiltonian as anti-polariton qubit Hamiltonian, then the time-dependent Schrödinger equation is used to calculate the time evolution of the anti JC model in the form

$$i\hbar\frac{\partial}{\partial(t)}|\Psi_{nd}\rangle = H_{aJC}|\Psi_{nd}\rangle \tag{3.0.1}$$

The state vector $|\Psi\rangle$ is taken to evolve from a spin-down state. Since anti polariton

Hamiltonian is time-independent, the time evolving state vector is evaluated in the form

$$|\Psi_{nd}(t)\rangle = U(t)|\Psi_{nd}\rangle \tag{3.0.2}$$

where

$$U(t) = e^{-\frac{i}{\hbar}H_{aJC}t} \tag{3.0.3}$$

Eq. (3.0.3) is the unitary time evolution equation.

3.1 Eigenvalue and eigenvectors of the anti JC model

We let the transition operator $\hat{\bar{A}}$ to act on state vector $|\Psi_{nd}\rangle$ to get

$$\hat{\bar{A}}|\Psi_{nd}\rangle = (\frac{\delta}{2g}\Omega_z + \hat{c}\Omega_- + \hat{c}^+\Omega_+)|nd\rangle \tag{3.1.1}$$

which by applying algebraic operations from Eq. (1.2.4) give

$$\hat{\bar{A}}|\Psi_{nd}\rangle = -\frac{1}{4}\frac{\delta}{g}|nd\rangle + \sqrt{n+1}|n+1u\rangle \tag{3.1.2}$$

simplified in the form

$$\begin{aligned} -\frac{1}{4}\frac{\delta}{g}|nd\rangle + \sqrt{n+1}|n+1u\rangle &= \sqrt{(-\frac{1}{4}\frac{\delta}{g})^2 + (\sqrt{n+1})^2} \\ &\quad \left(-\frac{-\frac{1}{4}\frac{\delta}{g}|nd\rangle + \sqrt{n+1}|n+1u\rangle}{\sqrt{(-\frac{1}{4}\frac{\delta}{g})^2 + (\sqrt{n+1})^2}}\right) \end{aligned} \tag{3.1.3}$$

we define probability amplitudes in the form

$$\chi_{n+1} = \frac{-\frac{1}{4}\frac{\delta}{g}}{\sqrt{(\delta)^2 + 16g^2(n+1)}} \tag{3.1.4}$$

and

$$\chi = \frac{\sqrt{n+1}}{\sqrt{(\delta)^2 + 16g^2(n+1)}} \tag{3.1.5}$$

we substitute Eq. (3.1.5) and Eq. (3.1.4) to Eq. (3.1.3) to obtain

$$\hat{\bar{A}}|nd\rangle = \sqrt{(\delta)^2 + 16g^2(n+1)}\{\chi_{n+1}|nd\rangle + \chi|n+1u\rangle\} \tag{3.1.6}$$

from Eq. (3.1.6) the state vector $|\Phi_{nd}\rangle$ is given by

$$|\Phi_{nd}\rangle = \chi_{n+1}|nd\rangle + \chi|n+1u\rangle \tag{3.1.7}$$

substituting Eq. (3.1.6) into Eq. (3.1.7) to get

$$\hat{\bar{A}}|\Psi_{nd}\rangle = \sqrt{\delta^2 + 16g^2(n+1)}|\Phi_{nd}\rangle \tag{3.1.8}$$

We then proceed by allowing the state transition operator $\hat{\bar{A}}$ to act on the state vector $|\Phi_{nd}\rangle$ defined in Eq. (2.3.2), in the form

$$\hat{\bar{A}}|\Phi_{nd}\rangle = \hat{\bar{A}}\{\chi_{n+1}|nd\rangle + \chi|n+1u\rangle\} = \chi_{n+1}(\hat{\bar{A}}|nd\rangle) + \chi(\hat{\bar{A}}|n+1u\rangle) \tag{3.1.9}$$

Since the first term on the right hand side of Eq. (3.1.9) had already been evaluated explicitly in Eq. (3.1.8), we evaluate the last term on the right hand side in the form

$$\hat{\bar{A}}|\Psi_{n+1d}\rangle = \frac{1}{2}\frac{\delta}{g}\Omega_z|n+1u\rangle + \hat{c}\Omega_-|n+1u\rangle + \hat{c}^+\Omega_+|n+1u\rangle \tag{3.1.10}$$

which on noting that

$$\hat{c}^+\Omega_+|n+1u\rangle = 0 \tag{3.1.11}$$

Equation (3.1.10) now takes the form

$$\hat{\bar{A}}|\Psi_{n+1d}\rangle = \frac{1}{4}\frac{\delta}{g}|n+1u\rangle + \sqrt{n+1}|nd\rangle \tag{3.1.12}$$

further expressible in the form

$$\begin{aligned}\hat{\bar{A}}|\Psi_{n+1d}\rangle \quad = \quad & \sqrt{(\delta)^2 + 16g^2(n+1)} \\ & \left(\frac{\frac{\delta}{4g}}{\sqrt{(\delta)^2 + 16g^2(n+1)}}|n+1u\rangle + \frac{\sqrt{n+1}}{\delta^2 + 16g^2(n+1)}|nd\rangle\right)\end{aligned} \tag{3.1.13}$$

From Eq. (3.1.4) and Eq. (3.1.5) it is easy to see that

$$\sqrt{n+1} = \chi\{\sqrt{(\delta^2 + 16g^2(n+1)}\} \tag{3.1.14}$$

and

$$\delta = -4g\chi_{n+1}\sqrt{\delta^2 + 16g^2(n+1)} \tag{3.1.15}$$

using Eq. (3.1.14) and Eq. (3.1.15) in Eq. (3.1.13) gives

$$\hat{\bar{A}}|\Phi_{nd}\rangle = \sqrt{\delta^2 + 16g^2(n+1)}|\Psi_{nd}\rangle \tag{3.1.16}$$

We observe that as expected the time evolving interaction variables $|\Psi_{nd}\rangle$ and $|\Phi_{nd}\rangle$ in this fully quantized electromagnetic field mode are quantized. In summary

$$\hat{\bar{A}}|\Psi_{nd}\rangle = \sqrt{\delta^2 + 16g^2(n+1)}|\Phi_{nd}\rangle \tag{3.1.17}$$

$$\hat{\hat{A}}|\Phi_{nd}\rangle = \sqrt{\delta^2 + 16g^2(n+1)}|\Psi_{nd}\rangle \tag{3.1.18}$$

We consider action of the transition operator on the state vector in the form

$$|\Psi^+\rangle = |\Psi_{nd}\rangle + |\Phi_{nd}\rangle \tag{3.1.19}$$

$$|\Psi^-\rangle = |\Psi_{nd}\rangle - |\Phi_{nd}\rangle \tag{3.1.20}$$

$$\hat{A}|\Psi^+\rangle = \sqrt{\delta^2 + 16g^2(n+1)}(|\Psi_{nd}\rangle + |\Phi_{nd}\rangle) \tag{3.1.21}$$

and

$$\hat{A}|\Psi^-\rangle = \sqrt{\delta^2 + 16g^2(n+1)}(|\Psi_{nd}\rangle - |\Phi_{nd}\rangle) \tag{3.1.22}$$

where $|\Psi^+\rangle$ and $|\Psi^-\rangle$ are the state eigenvectors of the anti JC Hamiltonian. It follows that

$$H_{aJC}|\Psi^+\rangle = \hbar\omega\hat{\hat{A}}^2|\Psi^+\rangle + 2\hbar g\hat{A}|\Psi^+\rangle - \frac{1}{4}\hbar\omega\frac{\delta^2}{g^2}|\Psi^+\rangle + \frac{1}{2}\hbar\omega|\Psi^+\rangle \tag{3.1.23}$$

giving

$$H_{aJC}|\Psi^+\rangle = \hbar\omega(n+\frac{3}{2}) + 2\hbar g\sqrt{\delta^2 + 16g^2(n+1)}|\Psi^+\rangle \tag{3.1.24}$$

which means that

$$\hbar\omega(n+\frac{3}{2}) + \hbar g\sqrt{\delta^2 + 16g^2(n+1)}|\Psi^+\rangle = E_{n^+}|\Psi^+\rangle \tag{3.1.25}$$

which implies that

$$H_{aJC}|\Psi^+\rangle = E_{n^+}|\Psi^+\rangle \tag{3.1.26}$$

and

$$H_{aJC}|\Psi^-\rangle = E_{n^-}|\Psi^-\rangle \tag{3.1.27}$$

where

$$E_{n^+} = \hbar\omega(n+\frac{3}{2}) + 2\hbar g\sqrt{\delta^2 + 16g^2(n+1)} \tag{3.1.28}$$

and

$$E_{n^-} = \hbar\omega(n+\frac{3}{2}) - 2\hbar g\sqrt{\delta^2 + 16g^2(n+1)} \tag{3.1.29}$$

We have derived the eigenvalue equations Eq. (3.1.28) and Eq. (3.1.29) of the anti JC model. The fact that the anti JC model has both eigenvalues and eigenvectors is enough prove that the anti JC model is exactly solvable.

3.2 Dynamical Evolution

The dynamical evolution of the polariton qubit states is generated by the polariton qubit state evolution operator. We start by writing the time-dependent Schrödinger equation in the form [21]

$$i\hbar\frac{\partial}{\partial t}|\Psi_{nd}\rangle = H_{aJC}|\Psi_{nd}\rangle \tag{3.2.1}$$

substituting Hamiltonian Eq. (1.4.5) into Eq. (3.0.3) provides the unitary time evolution operator in a factorized form

$$U(t) = e^{-i\omega(n+1)\frac{3}{2}It}e^{-iR_{n+1}\hat{\epsilon}t} \tag{3.2.2}$$

We proceed to investigate the algebraic properties of the anti polariton state vector in the form

$$\hat{\epsilon}^{+} = \hat{\epsilon} \quad ; \quad \hat{\epsilon}^{2} = I \quad ; \quad \hat{\epsilon}^{2k} = \hat{I} \quad ; \quad \hat{\epsilon}^{2k+1} = \hat{\epsilon} \quad ; \quad k = 0, 1, 2, 3.......... \tag{3.2.3}$$

$$e^{\pm i\theta\hat{I}} = e^{\pm i\theta}I \qquad ; \qquad e^{\pm i\theta\hat{\epsilon}} = \cos\theta\hat{I} \pm i\sin\theta\hat{\epsilon} \tag{3.2.4}$$

leading to

$$U(t) = e^{-iR_{n+1}\hat{\epsilon}t} = \sum_{k=0}^{\infty}\frac{(-i\beta t)^{k}}{k!}\hat{\epsilon}^{k} \tag{3.2.5}$$

where

$$e^{\beta\hat{\epsilon}} = \sum_{k=0}^{\infty}\frac{(\beta)^{k}}{k!}\hat{\epsilon}^{k} \tag{3.2.6}$$

which implies that

$$U(t)|\Psi_{nd}\rangle = \sum_{k=0}^{\infty}\frac{(-i\beta t)^{k}}{k!}\hat{\epsilon}^{k}|\Psi_{nd}\rangle \tag{3.2.7}$$

We solve Eq. (3.2.7) using exponential expansion where odd terms are grouped together and even terms also grouped together in the form

$$U(t)|\Psi_{nd}\rangle = (\sum_{k=0}^{\infty}\frac{(-iR_{n+1}t)^{2k}}{(2k)!}\hat{\epsilon}^{2k} + \sum_{k=0}^{\infty}\frac{(-iR_{n+1}t)^{2k+1}}{(2k+1)!}\hat{\epsilon}^{2k+1})|\Psi_{nd}\rangle \tag{3.2.8}$$

by applying

$$\hat{\epsilon}^{2k}|\Psi_{nd}\rangle = |\Psi_{nd}\rangle \quad ; \quad \hat{\epsilon}^{2k+1}|\Phi_{nd}\rangle = |\Phi_{nd}\rangle \tag{3.2.9}$$

it is now easy to see that

$$U(t)|\Psi_{nd}\rangle = \sum_{k=0}^{\infty}\frac{(-iR_{n+1}t)^{2k}}{(2k)!}\hat{\epsilon}^{2k}|\Psi_{nd}\rangle + \sum_{k=0}^{\infty}\frac{(-iR_{n+1}t)^{2k+1}}{(2k+1)!}\hat{\epsilon}^{2k+1}|\Phi_{nd}\rangle \tag{3.2.10}$$

further expressed in the form

$$U(t)|\Psi_{nd}\rangle = \sum_{k=0}^{\infty}\frac{(-i)^k(R_{n+1}t)^{2k}}{(2k)!}\hat{\epsilon}^{2k}|\Psi_{nd}\rangle - \sum_{k=0}^{\infty}\frac{(-i)^k(R_{n+1}t)^{2k+1}}{(2k+1)!}\hat{\epsilon}^{2k+1}|\Phi_{nd}\rangle \tag{3.2.11}$$

by letting

$$\sum_{k=0}^{\infty}\frac{(-i)^k(R_{n+1}t)^{2k}}{(2k)!}\hat{\epsilon}^{2k}|\Psi_{nd}\rangle = \cos(R_d t) \tag{3.2.12}$$

$$\sum_{k=0}^{\infty}\frac{(-i)^k(R_{n+1}t)^{2k+1}}{(2k+1)!}\hat{\epsilon}^{2k+1}|\Phi_{nd}\rangle = \sin(R_d t)$$

which now gives

$$U(t)|\Psi_{nd}\rangle = \cos(R_{n+1}t) - i\sin(R_{n+1}t) \tag{3.2.13}$$

We use the time evolution operator $U(t)$ to explicitly determine the general time evolving anti-polariton qubit state vectors starting from spin down state $|nd\rangle$, the general time evolving anti-polariton qubit state vectors $|\Psi_{nd}(t)\rangle$ and $|\Phi_{nd}(t)\rangle$ are generated from the respective initial qubit state vectors $|\Psi_{nu}(t)\rangle$ and $|\Phi_{nu}(t)\rangle$ through the respective time evolution operators according to

$$|\Psi_{nd}(t)\rangle = U(t)|\Psi_{nd}(t)\rangle \quad ; \quad |\Phi_{nd}(t)\rangle = U(t)|\Phi_{nd}(t)\rangle \tag{3.2.14}$$

implying that

$$|\Psi_{nd}(t)\rangle = e^{-i\omega(n+\frac{3}{2})t}\{\cos(R_{n+1}(t))|\Psi_{nd}\rangle - i\sin(R_{n+1}(t))|\Phi_{nd}\} \tag{3.2.15}$$

$$|\Phi_{nd}(t)\rangle = e^{-i\omega(n+\frac{3}{2})t}\{\cos(R_{n+1}(t))|\Phi_{nd}\rangle - i\sin(R_{n+1}(t))|\Psi_{nd}\} \tag{3.2.16}$$

but

$$|\Phi_{nd}\rangle = \chi_{n+1}|nd\rangle + \chi|n+1u\rangle \tag{3.2.17}$$

which we substitute back to obtain $|\Psi_{nd}(t)\rangle$ explicitly in the form

$$|\Psi_{nd}(t)\rangle = e^{-i\omega(n+\frac{3}{2})t}(\cos(R_{n+1}(t)) - i\chi_{n+1}\sin(R_{n+1}(t))|nd\rangle - i\chi\sin(R_{n+1}(t))|n+1u\rangle \tag{3.2.18}$$

3.3 Algebraic Properties of Qubit State Vectors

We determine if time-evolving anti-polariton qubit state vectors $|\Psi_{nu}(t)\rangle$ and $|\Phi_{nu}(t)\rangle$ obtained above preserve the normalization and non-orthogonality and state-transition algebraic relation of the qubit state vectors in the form [23]

$$\langle\Psi_{nd}(t)|\Psi_{nd}(t)\rangle = 1 \tag{3.3.1}$$

$$\langle\Phi_{nd}(t)|\Phi_{nd}(t)\rangle = 1 \tag{3.3.2}$$

We continue to investigate the non-orthogonality of the state vectors in the form

$$\langle\Psi_{nd}(t)|\Phi_{nd}(t)\rangle \tag{3.3.3}$$

On substituting (3.2.16) and (3.2.15) into (3.3.3), noting that $\cos^2_{n+1} + \sin^2_{n+1} = 1$ gives

$$\langle\Psi_{nd}(t)|\Phi_{nd}(t)\rangle = -\chi_{n+1} \tag{3.3.4}$$

We have explicitly established that the polariton qubit state vectors are non-orthogonal and normalized according to the relation

$$\langle\Psi_{nd}(t)|\Phi_{nd}(t)\rangle = -\chi_{n+1} \qquad ; \qquad \langle\Psi_{nd}(t)|\Psi_{nd}(t)\rangle = 1 \tag{3.3.5}$$

We observe the general time evolving state vectors to be entangled and preserve the normalization and non-orthogonality relations according to Eq. (3.3.5).

3.4 Dynamics of the anti JC model

We apply operator ordering as a fundamental algebraic property to determine the dynamics of the anti JC model. We start by calculating mean photon number which plays a fundamental role in the characterization of the light states, it is calculated in form

$$\overline{n} = \frac{\langle\Psi_{nd}(t)|\hat{n}|\Psi_{nd}(t)\rangle}{\langle\Psi_{nd}(t)|\Psi_{nd}(t)\rangle}. \tag{3.4.1}$$

but

$$\langle\Psi_{nd}(t)|\Psi_{nd}(t)\rangle = 1 \tag{3.4.2}$$

hence

$$\overline{n} = \langle \Psi_{nd}(t)|\hat{n}|\Psi_{nd}(t)\rangle. \tag{3.4.3}$$

We proceed to calculate the mean fluctuation which is used in the determination of the statistical properties of the model

$$\triangle\overline{n}(t) = \sqrt{\overline{n^2}(t) - (\overline{n}(t))^2} \tag{3.4.4}$$

We again proceed by noting that the mean value of the atomic spin population inversion Ω_z in the general time evolving state $|\Psi(t)\rangle$ constitutes the atomic spin population inversion in the form

$$\overline{\Omega_z}(t) = \frac{\langle \Psi_{nd}(t)|\Omega_z|\Psi_{nd}(t)\rangle}{\langle \Psi_{nd}(t)|\Psi_{nd}(t)\rangle} \tag{3.4.5}$$

hence

$$\overline{\Omega_z}(t) = \langle \Psi_{nd}(t)|\Omega_z|\Psi_{nd}(t)\rangle \tag{3.4.6}$$

After calculating the mean photon fluctuation we can easily calculate atomic inversion fluctuations in the form

$$\triangle\overline{\Omega_z}(t) = \sqrt{\overline{\Omega_z^2}(t) - (\overline{\Omega_z}(t))^2} \tag{3.4.7}$$

After explicit determination of the mean photon number and its fluctuation, spin atomic inversion and its fluctuation. We then plot the results to analyze the nature of the graphs.

3.5 Statistical properties of the anti JC interaction

We shall use the results obtained for the mean photon number to study photon statistics. Depending on the light source three regimes of statistical distribution can be obtained, poissonian or non-poissonian or super-poissonian. [49].

We finally calculate the reduced density matrix using the state vectors, this provide a useful way to characterize the state of the ensemble of quantum system given in the form

$$\rho(t) = |\Psi(t)_{nd}\rangle\langle\Psi(t)_{nd}|. \tag{3.5.1}$$

After developing the reduced density matrix, will then use it to generate the Bloch vector [57] which will be used to study the state of the atom, if the length of the state vector equals 1 then the atom is in pure state but if its ≤ 1 then the atom is in mixed state [58].

Chapter 4

Results and Discussion

4.1 Mean Photon Number

The mean photon number is an important figure of merit for the characterization of the light states. from Eq. (3.4.1), Eq. (3.4.2) and Eq. (3.4.3), it follows that

$$\begin{aligned}\hat{n}|\Psi_{nd}(t)\rangle &= e^{-i\omega(n+\frac{3}{2})t}\Big\{\cos(R_{n+1}t) - i\chi_{n+1}\sin(R_{n+1}t)\hat{c}\hat{c}^{+}|nd\rangle \\ &\quad -i\sin(\cos(R_{n+1}t))\hat{c}\hat{c}^{+}|n+1u\rangle\Big\} \qquad (4.1.1)\end{aligned}$$

expressible in the form

$$\begin{aligned}\hat{n}|\Psi_{nd}\rangle &= e^{-i\omega(n+\frac{3}{2})t}\Big\{(n+1)\cos(R_{n+1}t) - i\chi_{n+1}\sin(R_{n+1}t)|nd\rangle \\ &\quad -i(n+2)\chi\sin(R_{n+1}t)|n+1u\rangle\Big\} \qquad (4.1.2)\end{aligned}$$

we then let

$$\mu(t) = \cos(R_{n+1}t) - i\chi_{n+1}\sin(R_{n+1}t) \;\; ; \;\; \nu(t) = -i\chi sin(R_{n+1}t) \qquad (4.1.3)$$

substituting Eq. (4.1.3) back to Eq. (4.1.2) gives

$$\hat{n}|\Psi_{nd}(t)|\rangle = e^{-i\omega(n+\frac{3}{2})t}\{(n+1)\mu(t)|nd\rangle + (n+2)\nu(t)|n+1u\rangle\} \qquad (4.1.4)$$

Taking the conjugation of $|\overline{\Psi}_{nd}(t)\rangle$ in Eq. (3.2.15)

$$\langle\Psi_{nd}(t)| = \{\mu^{*}(t)\langle nd| + \nu^{*}(t)\langle n+1u|\}e^{i\omega(n+\frac{3}{2})t} \qquad (4.1.5)$$

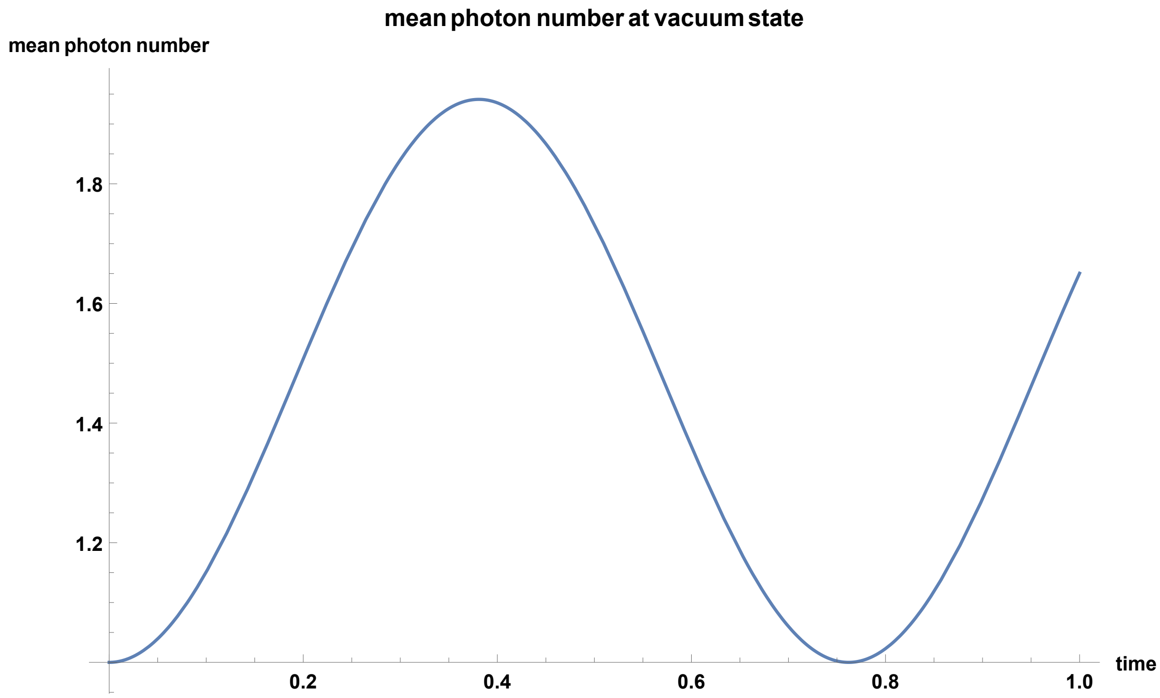

Figure 4.1: Mean photon number at n=0, time=1s

which now implies that

$$\langle \Psi_{nd}(t)|n|\Psi_{nd}(t)\rangle = (n+1)|\mu(t)|^2 + (n+2)|\nu(t)|^2 \tag{4.1.6}$$

which on further simplification taking note that $|\mu(t)|^2 + |\nu(t)|^2 = 1$ gives

$$\overline{n}(t) = n + 1 + |\nu(t)|^2 \tag{4.1.7}$$

substituting $\nu(t)$ from Eq. (4.1.3) into Eq. (4.1.7) gives the form

$$\overline{n}(t) = n + 1 + \chi^2 \sin^2(R_{n+1}t) \tag{4.1.8}$$

The mean photon number in Eq. (4.1.8) is time-dependent as expected. Setting $n = 0$ reveals that the anti JC interaction leads to an excitation of the quantized field mode vacuum state.

From Fig. (4.2), Fig. (4.3), Fig. (4.4), it is clear that all the graphs starts from the origin meaning ground state and evolves with time . The photon is seen to undergo periodic changes across the three displays, though at the vacuum state the oscillation is not much faster compared to when $n = 50$. This is because, the stronger the field, the size of the transition matrix elements also in turn increases and this makes the evolution to be

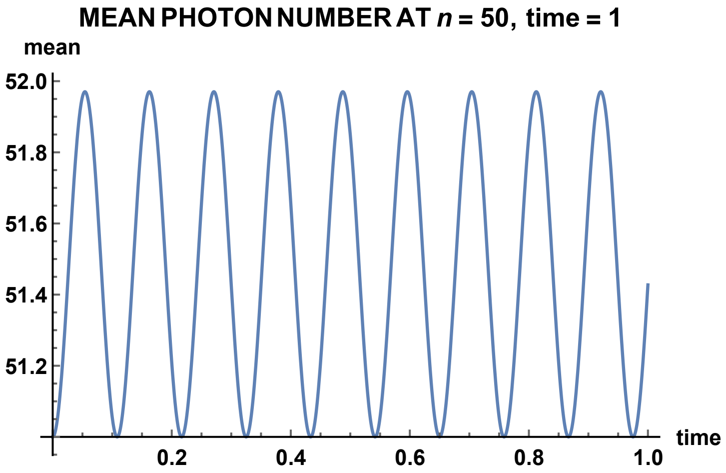

Figure 4.2: Mean photon number at n=50, time=1s

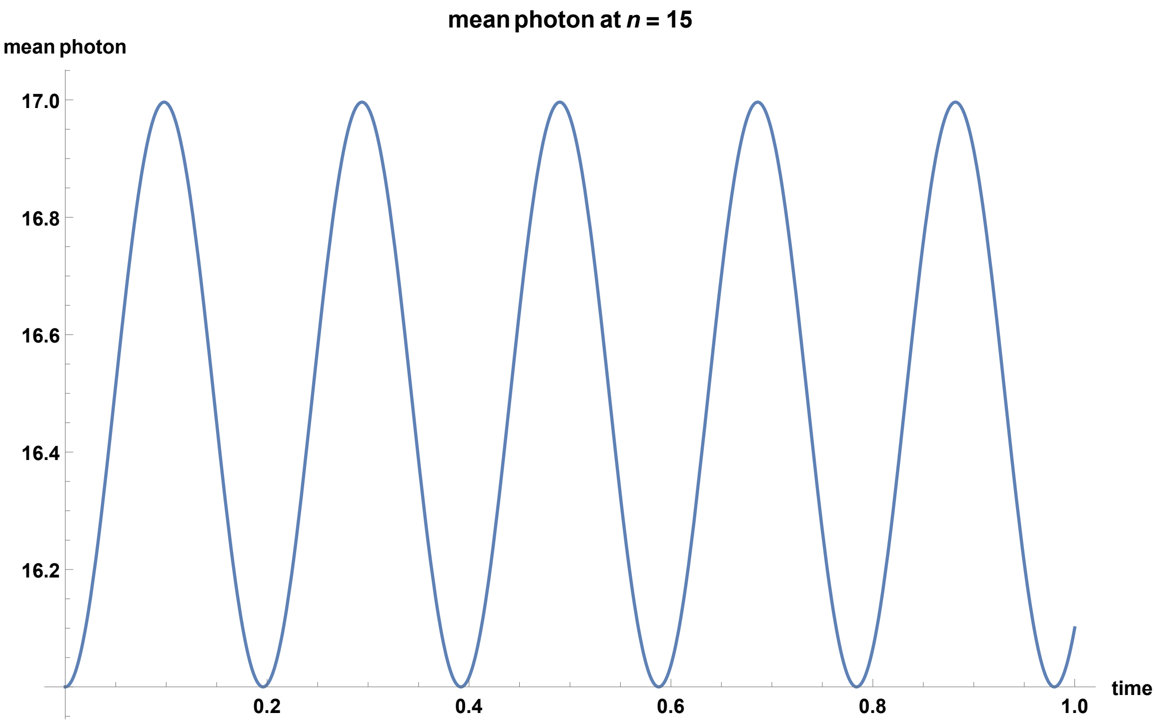

Figure 4.3: Mean photon number at n=15, time=1s

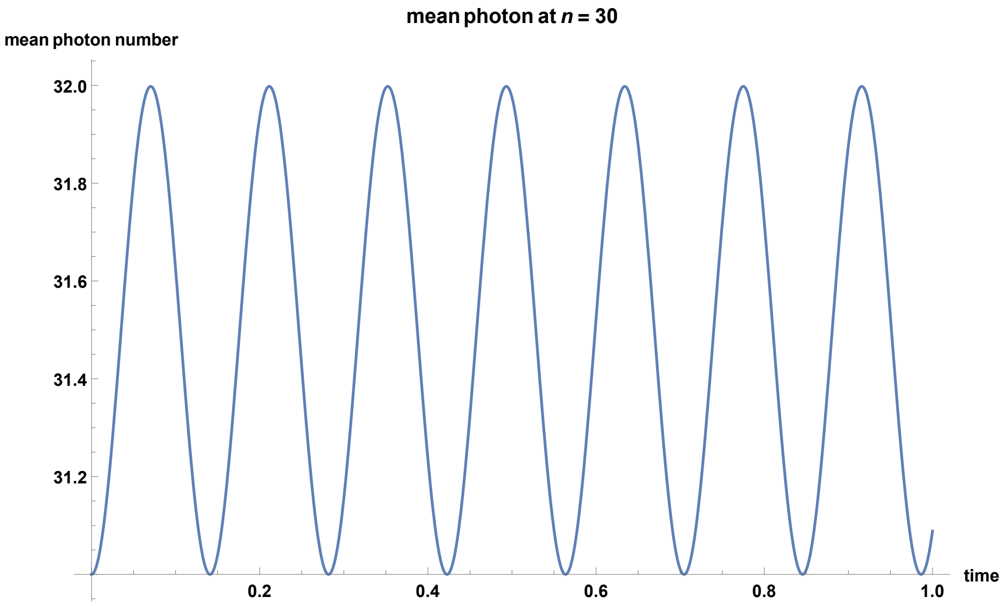

Figure 4.4: Mean photon number at n=30, time=1s

faster. More detailed comparison of the behavior of photons and atoms are explicitly explained in 4.2.

4.2 Fluctuations in Mean Photon Number

In quantum optics, fluctuations in mean photon number is calculated in [20]

$$\triangle\overline{n}(t) = \sqrt{\overline{n^2}(t) - (\overline{n}(t))^2} \tag{4.2.1}$$

We proceed to calculate the mean square photon number $\overline{n^2}(t)$ in the form

$$\overline{n^2}(t) = \langle\Psi_{nd}(t)|\overline{n^2}|\Psi_{nd}(t)\rangle \quad ; \quad \hat{n} = \hat{c}\hat{c}^{+} \quad ; \quad \hat{n}^2 = \hat{c}^2\hat{c}^{+2} \tag{4.2.2}$$

$$\overline{n^2}(t) = \langle\Psi_{nd}(t)|\hat{c}^2\hat{c}^{+2}|\Psi_{nd}(t)\rangle + \langle\Psi_{nd}(t)|\hat{c}\hat{c}^{+}|\Psi_{nd}(t)\rangle \tag{4.2.3}$$

which further takes the form

$$\overline{n^2}(t) = \langle\Psi_{nd}(t)|\hat{c}^2\hat{c}^{+2}|\Psi_{nd}(t)\rangle + \overline{n}(t) \tag{4.2.4}$$

We solve $\langle\Psi_{nd}(t)|\hat{c}^2\hat{c}^{+2}|\Psi_{nd}(t)\rangle$ in the form

$$\begin{aligned}\langle\Psi_{nd}|\hat{c}^2\hat{c}^{+2}|\Psi_{nd}\rangle \quad &= \quad (\mu^*(t)\langle nd| + \nu^*(t)\langle n+1u|) \\ &\quad\ \hat{c}^2\hat{c}^{+2}(\mu(t)|nd\rangle + \nu(t)|n+1u\rangle)\end{aligned} \tag{4.2.5}$$

further expressible in the form

$$\begin{aligned}\langle\Psi_{nd}|\hat{c}^2\hat{c}^{+2}|\Psi_{nd}\rangle &= (\mu^*(t)\langle nd| + \nu^*(t)\langle n+1u|) \\ &\quad (n(n-1)\mu(t)|nd\rangle + \nu(t)n(n+1)|n+1u\rangle)\end{aligned} \tag{4.2.6}$$

We obtain

$$\langle\Psi_{nd}(t)|\hat{c}^2\hat{c}^{+2}|\Psi_{nd}(t)\rangle = n(n-1)|\mu(t)|^2 + n(n+1)|\nu(t)|^2 \tag{4.2.7}$$

which we express in the form

$$\langle\Psi_{nd}(t)|\hat{c}^2\hat{c}^{+2}|\Psi_{nd}(t)\rangle = n^2 - n(|\mu(t)|^2 - |\nu(t)|^2) \tag{4.2.8}$$

Substituting Eq. (4.2.8) back into Eq. (4.2.4) gives

$$\overline{n^2}(t) = n^2 - n(|\mu(t)|^2 - |\nu(t)|^2) + \overline{n} \tag{4.2.9}$$

Using Eq. (4.2.9) in Eq. (4.2.1) gives the photon number fluctuations in the form

$$\triangle\overline{n}(t) = \sqrt{n^2 - n(|\mu(t)|^2 - |\nu(t)|^2) + \overline{n} - (\overline{n}(t))^2} \tag{4.2.10}$$

simplified further in the form

$$\triangle\overline{n}(t) = \sqrt{\overline{n}(t)(1-\overline{n}(t)) + n(n - |\mu|^2 + |\nu|^2)} \tag{4.2.11}$$

Factoring out $\sqrt{\overline{n}(t)}$ gives the form

$$\triangle\overline{n}(t) = \sqrt{\overline{n}(t)}\sqrt{(1-\overline{n}(t)) + \frac{n(n-|\mu|^2+|\nu|^2)}{\overline{n}(t)}} \tag{4.2.12}$$

where the factor

$$\sqrt{(1-\overline{n}(t)) + \frac{n(n-|\mu|^2+|\nu|^2)}{\overline{n}(t)}} \tag{4.2.13}$$

leads to the interpretation that the process takes non-poisonian statistics. In Fig. (4.8), Fig. (4.9), Fig. (4.7), Fig. (4.6), Fig. (4.5) the photon displays the same periodic behavior as mean photon number and oscillate much faster at the same photon state. Much details on whether the model is poisonian, non-poisonian or super-poisonian is explained in 4.2.1.

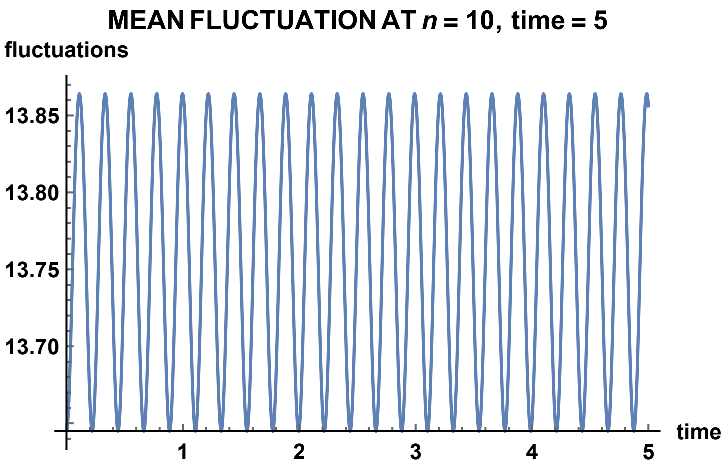

Figure 4.5: Mean fluctuation when n=10,time=5s

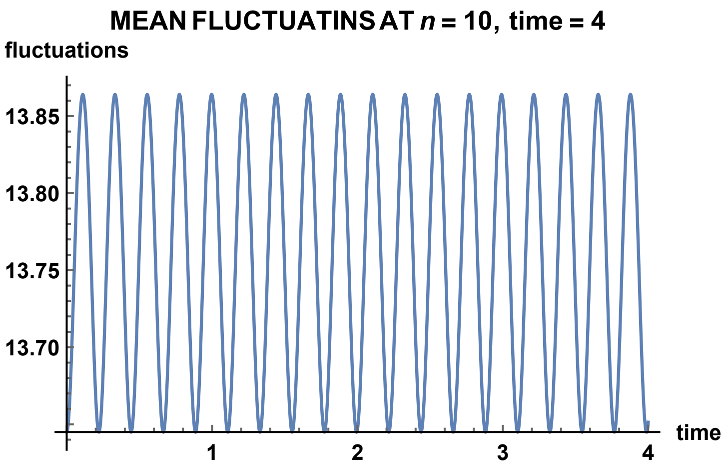

Figure 4.6: Mean fluctuation at n=10,time=4s

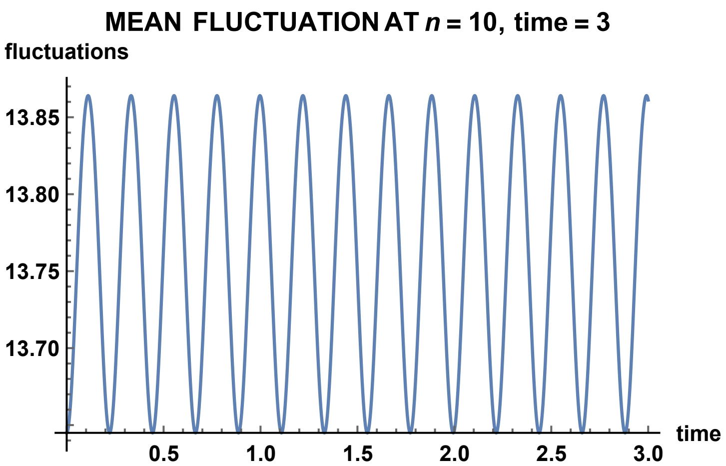

Figure 4.7: Mean fluctuation at n=10,time=3s

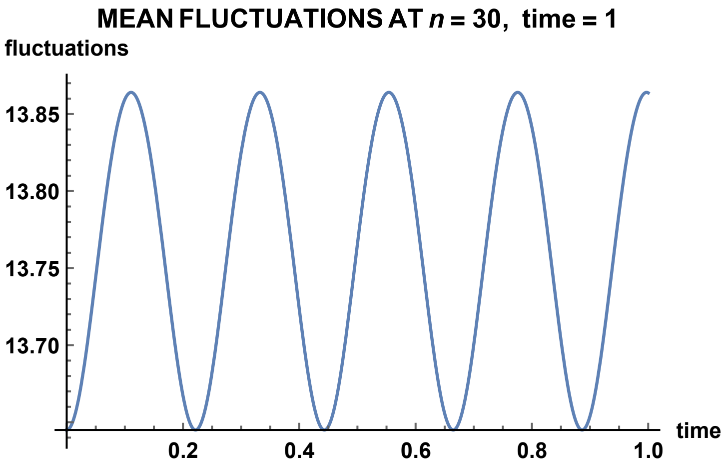

Figure 4.8: Mean fluctuation at n=10,time=1s

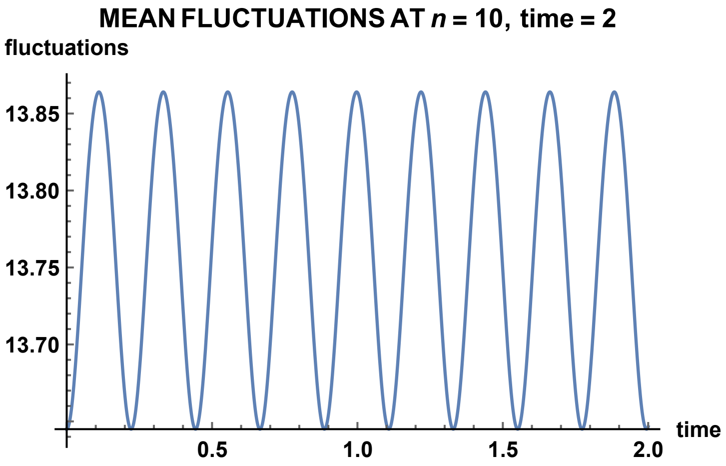

Figure 4.9: Mean fluctuation at n=10,time=2s

4.2.1 Mandel's Factor

We then proceed to examine the statistical properties of the anti JC model by comparing the results obtained for the mean photon number and its fluctuations by using Mandel's theory. Mandel's theory [49] applies to any kind of linearly polarized incident light, irrespective of its statistical properties or irrespective of whether light fluctuations are statistically stationary or not. The theory states that

$$Q = \frac{(\triangle\overline{n}(t))^2}{\overline{n}(t)} - 1 \tag{4.2.14}$$

From the Mandel's factor, one can obtain different types of statistical regimes that is Poisonian, super-poisonian and sub-poisonian regimes. We proceed by substituting the results obtained for the mean and its fluctuation in Eq. (4.1.8) and Eq. (4.2.12) respectively into Eq. (4.2.14) to obtain

$$Q = \frac{\overline{n}(t)(1-\overline{n}(t)) + n(n-|\mu|^2-|\nu|^2)}{n+1+|\nu(t)|^2} - 1 \tag{4.2.15}$$

By considering the initial field mode vacuum state $n = 0$ in Eq.(4.2.15) results to

$$Q_0 = \frac{\overline{n_0}(t)(1-\overline{n_0}(t)) + 0}{\overline{n_0}(t)} - 1 \tag{4.2.16}$$

meaning at $n = 0$

$$Q_0 = 1 - \overline{n_0}(t) - 1 = -\overline{n_0}(t) \tag{4.2.17}$$

Hence, in the initial field mode vacuum state $n = 0$, the Mandel's factor Q is given by:

$$Q_0 = -\overline{n_0}(t) \tag{4.2.18}$$

but from Eq. (4.1.8), taking $n = 0$ gives

$$\overline{n_0}(t) = 1 + |\nu(t)|^2 \tag{4.2.19}$$

which we substitute into Eq. (4.2.18) to get

$$Q_0 = -1 - |\nu(t)|^2 \tag{4.2.20}$$

Substituting $\nu(t)$ from Eq.(4.1.3) for $n = 0$ into Eq.(4.2.20) gives

$$Q_0 = -1 - \chi\sin^2(R_1 t) \tag{4.2.21}$$

We now proceed to consider Mandel's factor at $n = 1$, by first noting that

$$-|\mu(t)|^2 - |\nu(t)|^2 = -(|\mu(t)|^2 + |\nu(t)|^2) = -1 \tag{4.2.22}$$

It follows that at $n = 1$

$$Q_1 = \frac{\overline{n_1}(t)(1 - \overline{n_1}(t)) + (1 - |\mu|^2 - |\nu|^2)}{2 + |\nu(t)|^2} - 1 \tag{4.2.23}$$

but we note that $n = 1$

$$\overline{n_1}(t) = 2 + |\nu(t)|^2 \tag{4.2.24}$$

which is substituted and expanded to get

$$Q_1 = \frac{-2 - 2|\nu(t)|^2 - |\nu(t)|^2 - |\nu(t)|^4}{2 + |\nu(t)|^2} - 1 \tag{4.2.25}$$

further simplified in the form

$$Q_1 = \frac{-2 - 3|\nu(t)|^2 - |\nu(t)|^4}{2 + |\nu(t)|^2} - 1 \tag{4.2.26}$$

which can be expressed in the form

$$Q_1 = -(\frac{2 + 3|\nu(t)|^2 + |\nu(t)|^4}{2 + |\nu(t)|^2} + 1) \tag{4.2.27}$$

We finally consider a case when $n = 2$ in the form

$$-|\mu(t)|^2 - |\nu(t)|^2 = -(|\mu(t)|^2 + |\nu(t)|^2) = -1 \tag{4.2.28}$$

it then follows that

$$Q_2 = \frac{\overline{n_2}(t)(1 - \overline{n_2}(t)) + 2}{2 + |\nu(t)|^2} - 1 \tag{4.2.29}$$

simplified to take the form

$$Q_2 = \frac{3 + |\nu(t)|^2(-2 - |\nu(t)|^2) + 2}{3 + |\nu(t)|^2} - 1 \tag{4.2.30}$$

expanded and simplified in the form

$$Q_2 = \frac{-6 - 3|\nu(t)|^2 - 2|\nu(t)|^2 - |\nu(t)|^4 + 2}{3 + |\nu(t)|^2} - 1 \tag{4.2.31}$$

simplified in the final form

$$Q_2 = \frac{-4 - 5|\nu(t)|^2 - |\nu(t)|^4)}{3 + |\nu(t)|^2} - 1 \tag{4.2.32}$$

can be simplified further in the form

$$Q_2 = -(\frac{4 + 5|\nu(t)|^2 + |\nu(t)|^4)}{3 + |\nu(t)|^2} + 1) \tag{4.2.33}$$

We finally consider a general case for n in the form

$$Q = \frac{\overline{n}(t)(1 - \overline{n}(t)) + n(n - |\mu|^2 - |\nu|^2)}{n + 1 + |\nu(t)|^2} - 1 \tag{4.2.34}$$

which is expressible in the form

$$Q = \frac{\overline{n}(t)(1 - \overline{n}(t))}{\overline{n}(t)} + \frac{n(n - |\mu|^2 - |\nu|^2)}{\overline{n}(t)} - 1 \tag{4.2.35}$$

simplified to take the form

$$Q = 1 - \overline{n}(t) + \frac{n(n - |\mu|^2 - |\nu|^2)}{\overline{n}(t)} - 1 \tag{4.2.36}$$

which on expansion and substitution takes the form

$$Q = -n - \chi^2 \sin^2(R_{n+1}t) + \frac{n^2 - n(\cos^2(R_{n+1}t) + \chi^2_{n+1} \sin^2(R_{n+1}t) + \chi^2 \sin^2(R_{n+1}t))}{\overline{n}(t)} - 1 \tag{4.2.37}$$

which on factorization takes the form

$$Q = -1 - n - \chi^2 \sin^2(R_{n+1}t) - \frac{n^2 - nsin^2(R_{n+1}t) - n(\cos^2(R_{n+1}t)}{n + 1 + sin^2(R_{n+1}t)} \tag{4.2.38}$$

which after noting that

$$\sin^2(R_{n+1}t) + \cos^2(R_{n+1}t) = 1 \tag{4.2.39}$$

now takes the form

$$Q = -1 - n - \chi^2 \sin^2(R_{n+1}t) - \frac{n(n-1)}{n + 1 + \chi^2 \sin^2(R_{n+1}t)} \tag{4.2.40}$$

Taking a final explicit form

$$Q = -\{1 + n + \chi^2 \sin^2(R_{n+1}t) + \frac{n(n-1)}{n + 1 + \chi^2 \sin^2(R_{n+1}t)}\} \tag{4.2.41}$$

The results obtained from Eq. (4.2.21), Eq. (4.2.27), Eq. (4.2.33) and Eq. (4.2.41) both have negative value meaning that the photon statistics is sub-poissonian in nature and hence the photons are produced in anti-bunches, one at a time and the process is known as photon anti-bunching. Photon anti-bunching generally refers to a light with photons more equally spaced than a coherent laser field.

From the results obtained for Mandel's factor, it is now clear that the anti JC is purely quantum.

4.3 Atomic Spin Population Inversion

Atomic inversion is the photon number probability weighted sum of oscillating terms. It can also be taken as the difference in probabilities for the atom to be in the excited and ground states as earlier predicted by the JC model [18]. The mean value of the atomic spin operator Ω_z in the general time evolving state $|\Psi(t)\rangle$ constitutes the atomic spin-population inversion. We therefore obtain it in the form [28]

$$\overline{\Omega_z}(t) = \frac{\langle\Psi_{nd}(t)|\Omega_z|\Psi_{nd}(t)\rangle}{\langle\Psi_{nd}(t)|\Psi_{nd}(t)\rangle} \quad ; \quad \langle\Psi_{nd}(t)|\Psi_{nd}(t)\rangle = 1 \tag{4.3.1}$$

we proceed to solve

$$\overline{\Omega_z}(t) = \langle\Psi_{nd}(t)|\Omega_z|\Psi_{nd}(t)\rangle \tag{4.3.2}$$

in the form

$$\Omega_z|\Psi_{nd}(t)\rangle = e^{-i\omega(n+\frac{3}{2})t}\{\mu(t)\Omega_z|nd\rangle + \nu(t)\Omega_z|n+1u\rangle\} \tag{4.3.3}$$

which gives

$$\Omega_z|\Psi_{nd}(t)\rangle = \frac{1}{2}e^{-i\omega(n+\frac{3}{2})t}\{-\mu(t)|nd\rangle + \nu(t)|n+1u\rangle\} \tag{4.3.4}$$

Taking the conjugation of $|\overline{\Psi}_{nd}(t)\rangle$ in Eq. (3.2.15)

$$\langle\Psi_{nd}(t)| = \mu^*(t)\langle nd| + \nu^*(t)\langle n+1u|e^{i\omega(n+\frac{3}{2})t} \tag{4.3.5}$$

implies that

$$\langle\Psi_{nd}(t)|\Omega_z|\Psi_{nd}(t)\rangle = \frac{1}{2}\{|\nu(t)|^2 - |\mu(t)|^2\} \tag{4.3.6}$$

meaning

$$\overline{\Omega_z}(t) = \frac{1}{2}\{|\nu(t)|^2 - |\mu(t)|^2\} \tag{4.3.7}$$

Using the definition of $\mu(t)$ and $\nu(t)$ Eq. (4.1.3) gives

$$|\mu(t)|^2 = \cos^2(R_{n+1}t) + \chi^2\sin^2(R_{n+1}t) \ ; \quad |\nu(t)|^2 = \chi^2 sin^2(R_{n+1}t) \tag{4.3.8}$$

We obtain

$$\frac{1}{2}(|\nu(t)|^2 - |\mu(t)|^2) = \frac{1}{2}((\Omega^2_{n+1} - \chi^2)\sin^2(R_{n+1}t) - \cos^2(R^2_{n+1})) \tag{4.3.9}$$

further simplified in the form

$$\overline{\Omega_z}(t) = \frac{1}{2}(\Omega^2_{n+1}\sin^2(R_{n+1}t) - \cos^2(R_{n+1}t) - \chi^2\sin^2(R_{n+1}t)) \tag{4.3.10}$$

Using χ^2 and $\chi_n + 1^2$ from Eq. (3.1.4) and Eq. (3.1.5) in Eq. (4.3.10) gives

$$\overline{\Omega_z}(t) = \frac{1}{2}(\frac{\delta^2 - 16g^2(n+1)}{\delta^2 + 16g^2(n+1)})\sin^2(R_{n+1}t) - \cos^2(R_{n+1}t) \tag{4.3.11}$$

Eq.(4.3.11) is the atomic spin population inversion expressed in its explicit form.

As predicted by the presence of the term $\chi^2 - \chi_{n+1}^2$ in Eq. (4.3.11), which tells us analytically that the Rabi Hamiltonian oscillates between the negative and the positive values. The same has been predicted numerically from the graphs of the atomic inversion. Just as expected, as the atom is emitted, a photon is absorbed and vice versa.

4.4 Fluctuation in Atomic Inversion

From the mean photon fluctuation we can easily calculate atomic inversion fluctuations in the form

$$\triangle\overline{\Omega_z}(t) = \sqrt{\overline{\Omega_z^2}(t) - (\overline{\Omega_z}(t))^2} \tag{4.4.1}$$

but as proved earlier

$$\overline{\Omega_z}(t) = \frac{1}{2}\{|\nu(t)|^2 - |\mu(t)|^2\} \tag{4.4.2}$$

which when squared takes the form

$$(\overline{\Omega_z}(t))^2 = \frac{1}{4}(|\nu(t)|^2 - |\mu(t)|^2)^2 \tag{4.4.3}$$

we then proceed to determine the mean square atomic inversion in the form

$$\hat{\Omega}_Z = \frac{1}{2}\hat{\delta}_z = \frac{1}{2}\begin{pmatrix} 1 & 0 \\ 0 & -1 \end{pmatrix} \tag{4.4.4}$$

which on squaring gives

$$\hat{\Omega}_{zZ}^{\ 2} = \frac{1}{2}\hat{\delta}_z^2 = \frac{1}{4}\begin{pmatrix} 1 & 0 \\ 0 & -1 \end{pmatrix}\begin{pmatrix} 1 & 0 \\ 0 & -1 \end{pmatrix} = \frac{1}{4}\begin{pmatrix} 1 & 0 \\ 0 & 1 \end{pmatrix} = \frac{1}{4}I \tag{4.4.5}$$

it therefore means that

$$\overline{\Omega_z^2}(t) = \langle\Psi_{nd}(t)|\overline{\Omega_z^2}|\Psi_{nd}(t)\rangle \tag{4.4.6}$$

$$\overline{\Omega_z^2}(t) = \frac{1}{4} \tag{4.4.7}$$

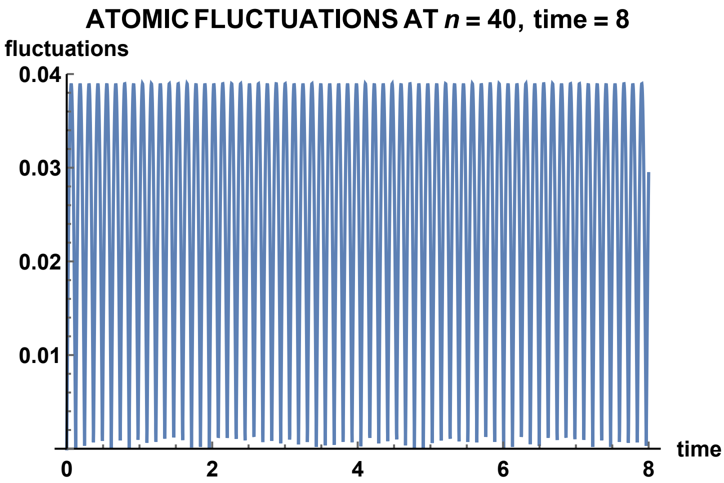

Figure 4.10: Atomic fluctuation at n=40,time=8s

meaning

$$\triangle\overline{\Omega_z}(t) = \frac{1}{4}(1-(|\mu|^2-|\nu|^2)^2) \tag{4.4.8}$$

meaning

$$\overline{\Omega_z^2}(t) - (\overline{\Omega_z}(t))^2 = \frac{1}{4} - (\overline{\Omega}(t))^2 \tag{4.4.9}$$

further implies that

$$\triangle\overline{\Omega_z}(t) = \frac{1}{2}\sqrt{1-(|\mu|^2-|\nu|^2)^2} \tag{4.4.10}$$

which now gives the atomic fluctuations in the final explicit form

$$\triangle\overline{\Omega_z}t = \frac{1}{2}\sqrt{1-((\Omega_{n+1}^2-\chi^2)\sin^2(R_{n+1}t)-\cos^2(R_{n+1}t))^2} \tag{4.4.11}$$

In Fig. (4.10), Fig. (4.11), Fig.(4.12), Fig. (4.17) Fig. (4.16), Fig. (4.18) shows the process through which atoms are emitted from the ground state as expected. Directly related to the atomic fluctuation is the mean fluctuations. They both show the same periodic behaviors. Fig. (4.13), Fig. (4.14), Fig. (4.15) clearly illustrates that fluctuations do not take place at vacuum state.

We have explicitly displayed the statistical and dynamical properties of the anti JC model by use of wolfram mathematica. We have taken the numerical path of solutions just to compare the behaviors we arrived at through the initial analytic method. It is clear that the numerical behaviors so far explained are the same with the analytical solutions as

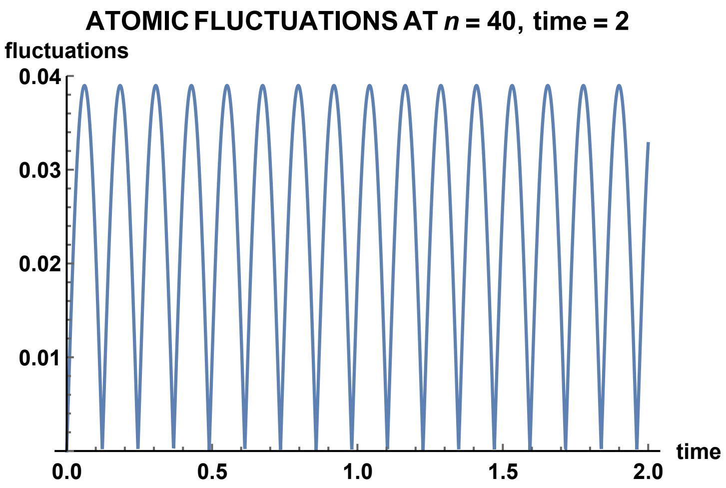

Figure 4.11: Atomic fluctuation at n=0,time=2s

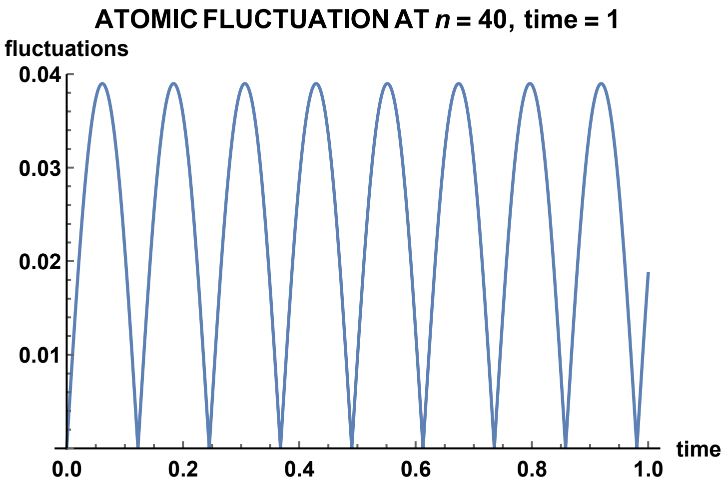

Figure 4.12: Atomic fluctuation at n=40,time=1s

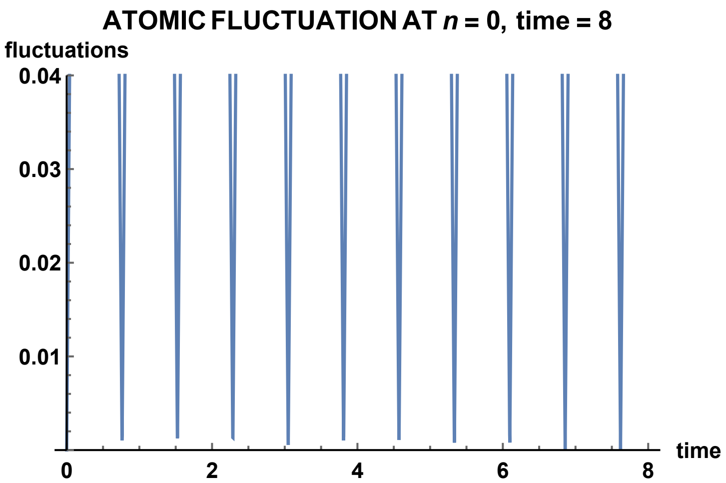

Figure 4.13: Atomic fluctuation at n=0,time=8s

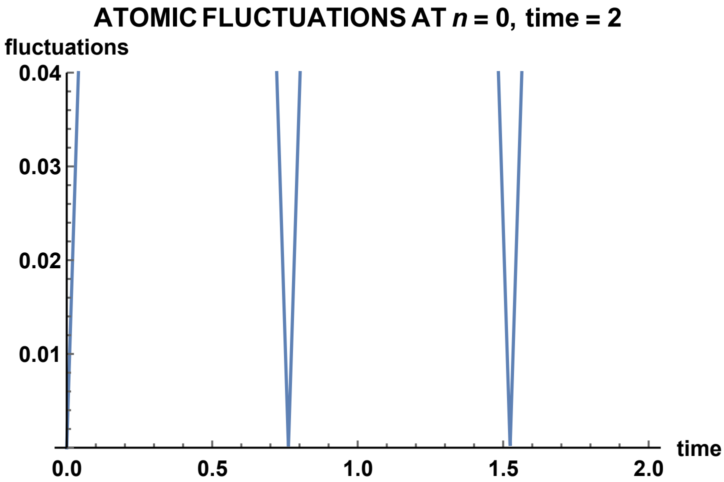

Figure 4.14: Atomic fluctuation at n=0,time=2s

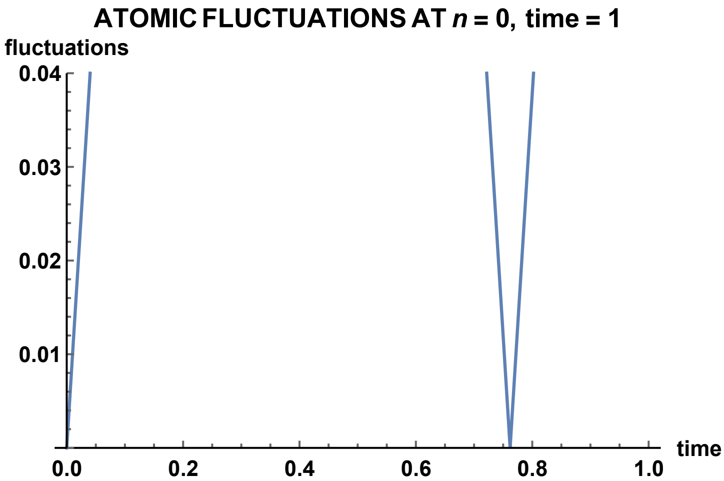

Figure 4.15: Atomic fluctuation at n=0,time=1s

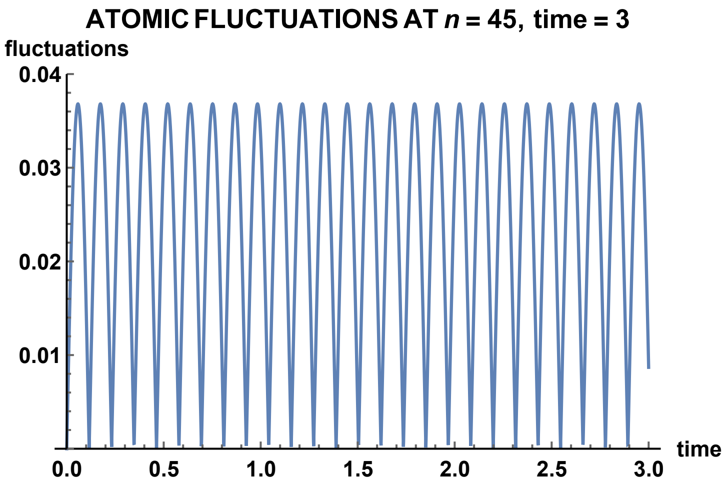

Figure 4.16: Atomic fluctuation at n=45,time=3s

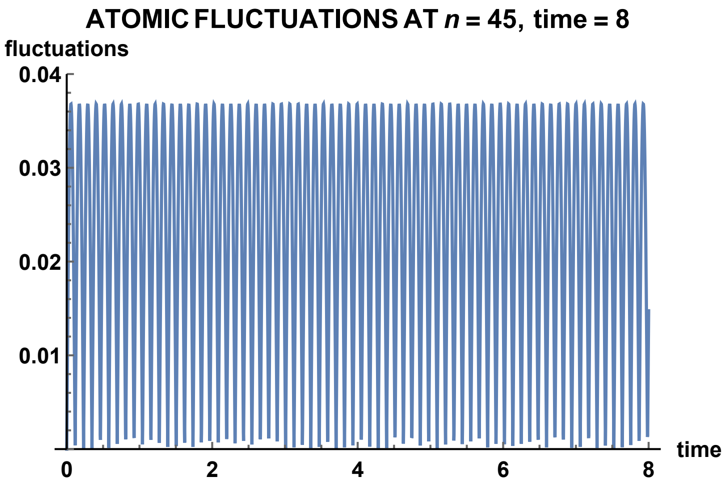

Figure 4.17: Atomic fluctuation at n=45,time=8s

expected. For example, we obtained numerically that the state is pure similar to the result obtained analytically.

4.5 Density Matrix

The density matrix denoted by $\rho(t)$ [25, 59, 60] provides a useful way to characterize the state of the ensemble of quantum system given in the form

$$\rho(t) = |\Psi(t)|\rangle\langle\Psi(t)| \tag{4.5.1}$$

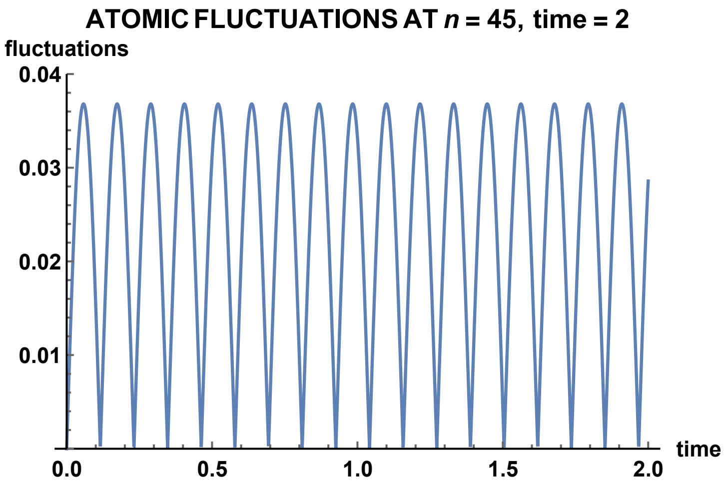

Figure 4.18: Atomic fluctuation at n=45,time=2s

which on substituting the time evolving state vector $|\Psi(t)\rangle$ which takes the form

$$|\Psi(t)\rangle = \cos(R_{n+1}t)|\Psi_{nd}\rangle - i\sin(R_{n+1}t|\Phi_{nd}\rangle) \tag{4.5.2}$$

gives

$$\begin{aligned} \rho(t) &= \{(\cos(R_{n+1}t)|\Psi_{nd}\rangle - (i\sin(R_{n+1}t))|\Phi_{nd}\rangle\} \\ &\quad \{(\cos(R_{n+1}t))\langle\Psi_{nd}| + (i\sin(R_{n+1}t))\langle\Phi_{nd}|\} \end{aligned} \tag{4.5.3}$$

evaluated to get

$$\begin{aligned} \rho(t) &= \cos^2(R_{n+1}t)|\Psi_{nd}\rangle\langle\Phi_{nd}| + i\cos(R_{n+1}t)\sin(R_{n+1}t)|\Psi_{nd}\rangle\langle\Phi_{nd}| \\ &\quad -i\sin(R_{n+1}t)\cos(R_{n+1}t)|\Psi_{nd}\rangle\langle\Phi_{nd}| + \sin^2(R_{n+1}t)|\Psi_{nd}\rangle\langle\Phi_{nd}| \end{aligned} \tag{4.5.4}$$

we then proceed by letting

$$\begin{aligned} \rho^{11}_{n+1}(t) &= \cos^2(R_{n+1}t) \\ \rho^{12}_{n+1}(t) &= i\cos(R_{n+1}t)\sin(R_{n+1}t) = \frac{1}{2}sin(2R_{n+1}t) \\ \rho^{21}_{n+1}(t) &= -i\sin(R_{n+1}t)\cos(R_{n+1}t) = -\frac{1}{2}\sin(2R_{n+1}t) \\ \rho^{22}_{n+1}(t) &= \sin^2(R_{n+1}t) \end{aligned} \tag{4.5.5}$$

We interpret the density operator $\rho(t)$ as elements of 2×2 density operator which we express in terms of the standard2×2 matrix $I, \sigma_x, \sigma_y, \sigma_z$ in the form

$$\rho_{n+1}(t) = \begin{pmatrix} \rho^{11}_{n+1}(t) & \rho^{12}_{n+1}(t) \\ \rho^{21}_{n+1}(t) & \rho^{22}_{n+1}(t) \end{pmatrix} \tag{4.5.6}$$

but

$$\rho^{11}_{n+1}(t) + \rho^{22}_{n+1}(t) = 1 \Rightarrow \rho_{n+1}(t) = \frac{1}{2}(I + \vec{\rho}_{n+1}(t).\vec{\sigma}) \tag{4.5.7}$$

Where we have introduced the Pauli spin matrix vector $\vec{\sigma}$ and a time evolving density vector $\vec{\rho}_{n+1}(t)$ defined by

$$\vec{\sigma} = (\sigma_x, \sigma_y, \sigma_z) \quad ; \quad \rho_{n+1}(t) = (\rho^x_{n+1}(t), \rho^y_{n+1}(t), \rho^z_{n+1}(t)) \tag{4.5.8}$$

where

$$\rho^x_{n+1} = \rho^{12}_{n+1}(t) + \rho^{21}_{n+1}(t) \ ; \ \rho^y_{n+1} = i(\rho^{12}_{n+1}(t) - \rho^{21}_{n+1}(t))$$

$$\rho^y_{n+1} = \rho^{11}_{n+1} + \rho^{22}_{n+1}(t) \tag{4.5.9}$$

Substituting the density matrix elements obtained earlier gives the components and length of the density matrix in the explicit form

$$\rho^x_{n+1} = \rho^{12}_{n+1}(t) + \rho^{21}_{n+1}(t) = 0 \tag{4.5.10}$$

$$\rho^y_{n+1}(t) = i(\rho^{12}_{n+1}(t) - \rho^{21}_{n+1}(t)) = i(\frac{i}{2}\sin(2R_{n+1}t) + \frac{i}{2}\sin(2R_{n+1}t))$$

hence

$$\rho^y_{n+1}(t) = -\sin(R_{n+1}t) \tag{4.5.11}$$

where we have used the trigonometric relation given by

$$\cos(2\alpha) = \cos^2\alpha - \sin^2\alpha \tag{4.5.12}$$

to obtain

$$\rho^z_{n+1}(t) = \cos(2R_{n+1})(t) = \cos(2R_{n+1}t) \tag{4.5.13}$$

giving

$$\vec{\rho}_{n+1}(t) = (\rho^x_{n+1}(t), \rho^y_{n+1}(t), \rho^z_{n+1}(t))$$

resulting to the density matrix in the final explicit form

$$\vec{\rho}_{n+1}(t) = (0, -\sin(2R_{n+1}t), cos(2R_{n+1}t)) \tag{4.5.14}$$

4.5.1 Length of Bloch Vector

$$|\vec{\rho}_{n+1}(t)| = \sqrt{(\sin(2R_{n+1}t))^2 + (\cos(2R_{n+1}t))^2} = \sqrt{1} \tag{4.5.15}$$

which gives the length of a Bloch vector in the final explicit form

$$|\vec{\rho}_{n+1}(t)| = 1 \tag{4.5.16}$$

The Bloch vector of a density matrix of the anti JC Hamiltonian is seen to have a unit length and is interpreted as the unit radius of a circle in the yz plane. This further implies that the model is in a pure state.

The process observed is purely quantum in nature and hence the model is very important for testing the prediction of quantum theory. Numerical solutions are also of great importance in the field of quantum information processing.

Chapter 5

Conclusion and Recommendations

5.1 Conclusion

In this Thesis, we applied the recently constructed excitation number operator[21, 23], to study the physical and statistical properties of the anti JC model, noting that similar studies have been successfully done on the JC model[61]. We have explicitly obtained the mean and its fluctautions which is then used in Mandel's factor to study the statistical properties of the anti-JC model. We have observed sub-poisonian statistics from the results obtained from Mandel's factor. This property reveals that the anti-Jaynes-Cummings interaction is characterize by photon anti-bunching process.

We have obtained the density operator which is then used in Bloch vector to study purity of state. The purity of state was shown by the Bloch sphere having a unit radius which demonstrates that the state generated in aJC is a pure state. The knowledge of quantized atom interacting with quantized light is fundamental in developing effective quantum computation protocols.

Theoretical adjustment in the aJC model will be important since approximations applied in the full Rabi model may be overlooked and the interaction taken strictly in the aJC interaction where now the effect of the negative component of the electromagnetic can now be implemented experimentally. Since it is still in the early stages of its development, it will be important to allow for new approaches in experimental realization if not observing the aJC interaction.

We have explicitly determine the statistical properties of the anti JC model. Attention can now be refocused on the study of the practical application of the anti JC model such as quantum computing and quantum teleportation.

5.2 Recommendations for further Research

We have explicitly obtained the dynamics of the anti JC model. Attention can now be refocused on the study of the practical application of the anti JC model such as quantum computing and quantum teleportation.

References

[1] Y. Salama and N. Gisin. Explicit examples of dissipative systems in the quantum state diffusion model. *Phys. Lett. A*, 181(4):269 – 275, 1993.

[2] B. R. Mollow. Power Spectrum of Light Scattered by Two-Level Systems. *Phys. Rev.*, 188:1969–1975, 1969.

[3] D. F. Walls and G. J. Milburn. *Quantum Optics*. Springer, 2008.

[4] B. Alberto and L. Giancarlo. Quantum stochastic models of two-level atoms and electromagnetic cross sections. *J. Math. Phys.*, 41(11):7181–7205, 2000.

[5] B. Heinz-Peter and P. Francesco. *The Theory of Open Quantum Systems*. Oxford University Press, 2007.

[6] D. F. Walls and P. Zoller. Reduced Quantum Fluctuations in Resonance Fluorescence. *Phys. Rev. Lett.*, 47:709–711, 1981.

[7] R. Xie, G. Xu, and D. Liu. Study of Some Properties of Two-Level Atom in Quantum Optics. *Commun. Theor. Phys.*, 27(3):265–278, 1997.

[8] I. I. Rabi. On the Process of Space Quantization. *Phys. Rev.*, 49:324–328, 1936.

[9] T. V . Foerster. A comparison of quantum and semi-classical theories of the interaction between a two-level atom and the radiation field. *J. Phys. A: Math. Gen.*, 8 (1):95–103, 1975.

[10] G. Wendin. Quantum information processing with superconducting circuits: a review. *Rep. Prog. Phys.*, 80(10):106001, 2017.

[11] M. A. Nielsen and Isaac L. Chuang. *Quantum Computation and Quantum Information: 10th Anniversary Edition.* Cambridge University Press, 2010.

[12] Lev Vaidman. Teleportation of quantum states. *Phys. Rev. A*, 49:1473–1476, 1994.

[13] Hong L. and G. Guo. Teleportation of a two-particle entangled state via entanglement swapping. *Phys. Lett. A*, 276(5):209 – 212, 2000.

[14] B. Shi and A. Tomita. Teleportation of an unknown state by W state. *Phys. Lett. A*, 296(4):161 – 164, 2002.

[15] N. David. *Quantum Computer Science: An Introduction.* Cambridge University Press, 2007.

[16] V. N. Gorbachev and A. I. Trubilko. Quantum teleportation of an Einstein-Podolsy-Rosen pair using an entangled three-particle state. *J. Exp. Theor. Phys.*, 91(5): 894–898, 2000.

[17] C. H. Bennett, B. Gilles, P. Claude, J. Richard, P. Asher, and W. K. William. Teleporting an unknown quantum state via dual classical and Einstein-Podolsky-Rosen channels. *Phys. rev. lett.*, 70(13):1895, 1993.

[18] E. T. Jaynes and F. W. Cummings. Comparison of quantum and semiclassical radiation theories with application to the beam maser. *Proc. IEEE.*, 51(1):89–109, 1963.

[19] E. Rubino, J. McLenaghan, S. C. Kehr, F. Belgiorno, D. Townsend, S. Rohr, C. E. Kuklewicz, U. Leonhardt, F. König, and D. Faccio. Negative-Frequency Resonant Radiation. *Phys. Rev. Lett.*, 108:253901, 2012.

[20] P. Meystre and M. Sargent III. *Elements of Quantum Optics.* Springer, 2007.

[21] J. A. Omolo. Conserved excitation number and U (1)-symmetry operators for the antirotating (anti-Jaynes-Cummings) term of the Rabi Hamiltonian. 2017. ResearchGate:10.13140/RG.2.2.30936.80647.

[22] C. Mayero, J. A. Omolo, and Onyango S. O. Rabi Oscillations, Entanglement and Teleportation in the Anti-Jaynes-Cummings Model. *J. Mod. Phys.*, 12:408–432, 2021.

[23] J. A. Omolo. Polariton and anti-polariton qubits in the Rabi model. 2017. ResearchGate:10.13140/RG.2.2.11833.67683.

[24] S. Schweber. On the application of Bargmann Hilbert spaces to dynamical problems. *Ann. Phys.*, 41(2):205 – 229, 1967.

[25] J. H. Eberly, N. B. Narozhny, and J. J. Sanchez-Mondragon. Periodic spontaneous collapse and revival in a simple quantum model. *Phys. Rev. Lett.*, 44:1323–1326, 1980.

[26] J. Casanova, G. Romero, I. Lizuain, J. J. García-Ripoll, and E. Solano. Deep Strong Coupling Regime of the Jaynes-Cummings Model. *Phys. Rev. Lett.*, 105:263603, 2010.

[27] R. Shankar. *Principles of Quantum Mechanics*. Springer Nature, 2 edition, 2020.

[28] J. J. Sakurai and N. Jim. *Modern Quantum Mechanics*. Cambridge University Press, 2nd edition, 2017.

[29] Y. Hardy and W.-H. Steeb. A Sequence of Quantum Gates. *Int. J. Geom. Methods Mod. Phys.*, 9(7):1220013, 2012.

[30] B. Max and W. Emil. *Principles of Optics (Electromagnetic Theory of Propagation, Interference and Diffraction of Light)*. Cambridge University Press, 1999.

[31] W. J. Baker, T. L. Keevers, J. M. Lupton, D. R. McCamey, and C Boehme. Slow hopping and spin dephasing of Coulombically bound polaron pairs in an organic semiconductor at room temperature. *Phys. rev. lett.*, 108(26):267601, 2012.

[32] F Y Sun, D Hou, Q S Bai, and X H Huang. Rabi resonance in cs atoms and its application to microwave magnetic field measurement. *J. Phys. Commun.*, 2(1): 015008, 2018.

[33] I. I. Rabi, J. R. Zacharias, M. Sidney, and K. Polykarp. A new method of measuring nuclear magnetic moment. *Phys. rev.*, 53(4):318, 1938.

[34] D. Raymond. Tumor detection by nuclear magnetic resonance. *Science*, 171(3976): 1151–1153, 1971.

[35] Y. Zhang, E. Lötstedt, and K. Yamanouchi. Population inversion in a strongly driven two-level system at far-off resonance. *J. Phys. B*, 50(18):185603, 2017.

[36] Loïc Henriet, Zoran Ristivojevic, Peter P. Orth, and Karyn Le Hur. Quantum dynamics of the driven and dissipative rabi model. *Phys. Rev. A*, 90:023820, Aug 2014.

[37] Mario F. Gely, P. Rodriguez, Adrian, Daniel Bothner, Ya. M. Blanter, Sal J. Bosman, Enrique Solano, and Gary A. Steele. Convergence of the multimode quantum rabi model of circuit quantum electrodynamics. *Phys. Rev. B*, 95(24), 2017.

[38] D. Braak. Integrability of the Rabi Model. *Phys. Rev. Lett.*, 107:100401, 2011.

[39] Q. X, Z. Honghua, M. T. Batchelor, and L. Chaohong. The quantum rabi model: solution and dynamics. *J. Phys A: Math. Theor.*, 50(11):113001.

[40] H. Rudolf and K. Daniel. An algebraic approach to quantum field theory. *J. Math. Phys.*, 5(7):848–861, 1964.

[41] P. A. M. Dirac. *The Principles of Quantum Mechanics.* Oxford University Press, 4th edition, 1958.

[42] G. Qin, K. Wang, T. Li, R. Han, and M. Feng. Stationary system of a two-level atom interacting with a single-mode phonon. *Phys. Lett. A*, 239(4):272–276, 1998.

[43] Y. Wang, W. You, M. Liu, Y. Dong, H. Luo, G Romero, and J Q You. Quantum criticality and state engineering in the simulated anisotropic quantum rabi model. *J. Phys.*, 20(5):053061, 2018.

[44] J. M. Raimond, M. Brune, and S. Haroche. Manipulating quantum entanglement with atoms and photons in a cavity. *Rev. Mod. Phys.*, 73:565–582, 2001.

[45] P. W. Milonni, J. R. Ackerhalt, and H. W. Galbraith. Chaos in the semiclassical n-atom jaynes-cummings model: Failure of the rotating-wave approximation. *Phys. Rev. Lett.*, 50(13):966, 1983.

[46] G. S. Agarwal. Vacuum-field rabi oscillations of atoms in a cavity. *J. Opt. Soc. Am. B*, 2(3):480–485, 1985.

[47] J. Gea-Banacloche. Loss of state purity and regularity in the jaynes-cummings model. *Phys. Rev. A*, 46:7307–7310, 1992.

[48] Roy J. Glauber. Coherent and Incoherent States of the Radiation Field. *Phys. Rev.*, 131:2766–2788, 1963.

[49] L. Mandel. Sub-Poissonian photon statistics in resonance fluorescence. *Opt. Lett.*, 47:205, 1979.

[50] D. T. Pegg, R. Loudon, and P. L. Knight. Correlations in light emitted by three-level atoms. *Phys. Rev. A*, 33:4085–4091, 1986.

[51] C. Emary and T. Brandes. Chaos and the quantum phase transition in the dicke model. *Phys. Rev. E*, 67:066203, 2003.

[52] T. Werlang, A. V. Dodonov, E. I. Duzzioni, and C. J. Villas-Bôas. Rabi model beyond the rotating-wave approximation: Generation of photons from vacuum through decoherence. *Phys. Rev. A*, 78:053805, 2008.

[53] R. H. Dicke. Coherence in Spontaneous Radiation Processes. *Phys. Rev.*, 93:99–110, 1954.

[54] L. Lamata, A. Rodriguez, M. Sanz, and E. Solano. Digital-analog quantum simulations with superconducting circuits. *Adv. Phys.: X*, 3(1):1457981, 2018.

[55] L. G. Lutterbach and L. Davidovich. Method for Direct Measurement of the Wigner Function in Cavity QED and Ion Traps. *Phys. Rev. Lett.*, 78:2547–2550, 1997.

[56] R Graham and M Höhnerbach. Quantum chaos of the two-level atom. *Phys. Lett. A*, 101(2):61–65, 1984.

[57] A. Hiroo. Dynamics of the Bloch vector in the thermal Jaynes-Cummings model. *Phys. Rev. A*, 77:063820, 2008.

[58] D. J. Wineland. Nobel Lecture: Superposition, entanglement, and raising Schrödinger's cat. *Rev. Mod. Phys.*, 85:1103–1114, 2013.

[59] U. Fano. Description of States in Quantum Mechanics by Density Matrix and Operator Techniques. *Rev. Mod. Phys.*, 29:74–93, 1957.

[60] P. Schneeweiss, A. Dareau, and C. Sayrin. Cold-atom-based implementation of the quantum Rabi model. *Phys. Rev. A*, 98:021801, 2018.

[61] B. W. Shore. Sir Peter Knight and the Jaynes–Cummings model. *J. Mod. Opt.*, 54 (13-15):2009–2016, 2007.